# Transitional adakite-like to calc-alkaline magmas in a continental extensional setting at La Paz Au-Cu skarn deposits, Mesa Central, Mexico: metallogenic implications

**Porfirio J. Pinto-Linares[1], Gilles Levresse[2,*], Jordi Tritlla[2], Víctor A. Valencia[3], José M. Torres-Aguilera[4], Manuel González[5], and David Estrada[5]**

*[1] Instituto Potosino de Investigación Científica y Tecnologica, División Geociencias Aplicadas, Camino a la Presa San José 2055, Col. Lomas 4ª Sección, 78216, San Luis Potosí, S.L.P., Mexico.*
*[2] Programa de Geofluidos, Centro de Geociencias Universidad Nacional Autónoma de México, Campus Juriquilla, Blvd. Villas del Mesón s/n, 76230 Querétaro, Qro., Mexico.*
*[3] Department of Geosciences, University of Arizona, 1040 East Fourth Street, Room 510, Tucson, Arizona 85721-0077, USA.*
*[4] Universidad Autónoma de San Luis Potosí, Depto. Ciencias de la Tierra, Dr. Manuel Nava 8, 78290 San Luis Potosí, S.L.P., Mexico.*
*[5] Negociación Minera Santa María de la Paz y Anexas, S.A. de C.V., 78830 Villa de La Paz, S.L.P., Mexico.*
** glevresse@geociencias.unam.mx*

**ABSTRACT**

*The granodiorite intrusions with associated Cu-Au skarn mineralization of La Paz district are located in the east part of the Mesa Central of Mexico. The skarn developed at the contact between a middle Cretaceous calc-argillaceous sedimentary sequence and the magmatic intrusions. A Ag-Pb-Zn vein system postdates the intrusive-skarn assemblage. Two well defined fault systems (N-S and E-W) divide the La Paz district. The N-S Dolores fault, with a normal vertical displacement estimated between 500 to 1000 m, separates the western Au-Cu skarn zone from the eastern hydrothermal Ag-Pb-Zn vein system. This fault is considered to be part of the Taxco-San Miguel de Allende fault system. The U-Pb dating of the intrusives at the La Paz district clearly indicates a single emplacement event dated at ca. 37 Ma (monocrystal zircon age). This age probably represents the last post-Laramide orogenic mineralizing event known to occur in the Sierra de Catorce district. Also, four calculated discordant ages suggest the presence of greenvilian basement underneath a a thick crust (35-45 km).*

*The chemistry of the intrusive show a certain variability in composition, but they mostly belong to the high-K calc-alkaline magmatic series. Major and trace elements relationships for the intrusives show a chemical evolution from the adakite to the island arc fields, and from mineralized to barren intrusives, repectively. They also suggest the importance of crustal delamination processes, and the necessity of deep cortical drains to transfer oxidized magmas and metals to surface.*

*Key words: Adakite-like, Au-Cu skarn, U-Pb, geochronology, geochemistry, La Paz, Mesa Central, Mexico.*

**RESUMEN**

*Las intrusiones granodioríticas que dieron origen a un depósito de Au-Cu tipo skarn en el distrito minero de La Paz, S.L.P., se localizan en la parte oriental de la Mesa Central. El skarn se desarrolló en el contacto entre una secuencia sedimentaria calco-argílica del Cretácico medio y los intrusivos. Un sistema de vetas mineralizadas en Ag-Pb-Zn post-datan el Skarn. El distrito de La Paz está dividido por dos sistemas de fallas muy bien definidas (N-S y E-W). La falla Dolores, de dirección N-S , muestra*

*un desplazamiento normal vertical estimado entre 500 a 1000 m y separa la zona occidental de skarn de Au-Cu de la zona oriental que contiene al sistema hidrotermal de vetas de Ag-Pb-Zn. Esta falla se considera como parte del sistema de fallas Taxco-San Miguel de Allende. El fechamiento de los intrusivos mediante el método U-Pb en circones indica claramente un único evento de emplazamiento alrededor de 37 Ma. Esta fecha representa el último de los pulsos mineralizantes, posteriores a la orogenia Laramide, reconocido en el distrito de la Sierra de Catorce. Asimismo se reportan cuatro edades discordantes que sugieren la presencia de rocas greenvilianas en la base de una corteza gruesa (35–45 km).*

*La geoquímica de los intrusivos muestra algunas diferencias en su composición, pero pertenecen a la serie magmática calco-alcalina con alto contenido de K. Los estudios de elementos mayores y traza muestran una evolución desde el campo adakítico hasta el campo de arco de islas, desde los intrusivos mineralizados a los estériles, respectivamente. Estos datos también sugieren la importancia del proceso de delaminación cortical y la necesidad de fallas profundas para transferir dicho magma y metales hacia la superficie.*

*Palabras clave: Adakite, Au-Cu skarn, U-Pb, geocronología, geoquímica, La Paz, Mesa Central, México.*

## INTRODUCTION

Intrusion-related hydrothermal systems obtain their thermal energy and variable amounts of volatiles, metals and other components largely from subduction-related magmas emplaced at shallow levels of the Earth's crust (Cathles 1981; Sawkins, 1990). Most of the Au-Cu-Ag-Pb-Zn profitable skarn deposits in the world are spatially related to porphyry copper deposits and alike. In western Mexico, this relationship has been repeatedly outlined by several authors (Clark *et al.*, 1982; Campa and Coney, 1984; Sillitoe and Gappe, 1984; Megaw *et al.*, 1988; Sawkins, 1990; Albinson and Nelson, 2001; Valencia-Moreno *et al.*, 2006). The "Copper Cluster", located between northwestern Mexico, Arizona and New Mexico (USA), is one of the most important copper accumulation on Earth, which may compete in size with the famous deposits of the Andes Cordillera of South America (Clark, 1993; Camus, 2003).

Most of the Mexican porphyry copper deposits (Cu-Au-Mo) are located in the eastern part of the Laramide magmatic belt (90–40 Ma). The largest and best preserved deposits outcrop in northeastern Sonora, where Cananea (~30 Mt Cu) and La Caridad (~8 Mt Cu) stand out as world-class ore deposits.

For the Andes deposits, Skewes and Stern (1994) suggested that exsolution of copper-bearing magmatic fluids were responsible for brecciation, alteration, and mineralization due to a rapid decrease of lithostatic pressure. In northern Mexico (Valencia-Moreno *et al.*, 2006), the association of Laramide deformation and magmatism is a consequence of the subduction regime, due to the radical change of the dip angle of the Farallon oceanic plate underneath the North America continental crust during Cretaceous-Tertiary ages. At the end of the Cretaceous, the angle of the subducted plate considerably diminished as result of the increase in the velocity of the converging plate, inducing the accelerated migration of the magmatic arc axis towards the east (Dickinson and Snyder, 1978; Clark *et al.*, 1982; Bird, 1988; Meschede *et al.*, 1997; Bunge and Grand, 2000).

Previous works on the La Paz deposit mainly focused on the origin and processes that led to the formation of the vein system, as well as on the characterization of the associated hydrothermal mineralization and alteration (Castro-Larragoitia, 1990). In this paper we study the geochemical composition of the porphyry intrusions associated with the Au-Cu skarn mineralization at the La Paz deposit, and discuss the possible magma sources and the interrelations between the skarn deposit and the vein system.

## GEOLOGICAL SETTING

The La Paz district is located in the eastern border of the Mesa Central, in central Mexico (Figure 1). The Mesa Central is an elevated plateau mainly covered by Cenozoic volcanic sequences, affected by the Eocene and Oligocene east-west extension (Nieto-Samaniego *et al.*, 2005) that created a series of deep continental basins filled with alluvial and lacustrine sediments. The eastern boundary of the Mesa Central is the Oligocene Taxco-San Miguel de Allende deep fault system. The major structure that separates the northern and southern regions of the Mesa Central is the San Luis-Tepehuanes fault system, that was active mostly between the Eocene and the Oligocene, but also during Pliocene-Quaternary times in its northwestern segment (Nieto-Samaniego *et al.*, 2005).

The oldest rocks exposed in the Mesa Central are represented by Triassic marine facies which are overlain, all along the Mesa Central, by lower and middle Jurassic continental rocks, mainly volcanics, conglomerates and sandstones, and an upper Jurassic to late Cretaceous marine sedimentary sequence. Cenozoic materials are mostly represented by conglomerates and volcanic rocks of andesitic to rhyolitic composition. The last Cenozoic magmatic felsic event is characterized by the presence of F-rich rhyolites with normative topaz (Orozco-Esquivel *et al.*, 2002).

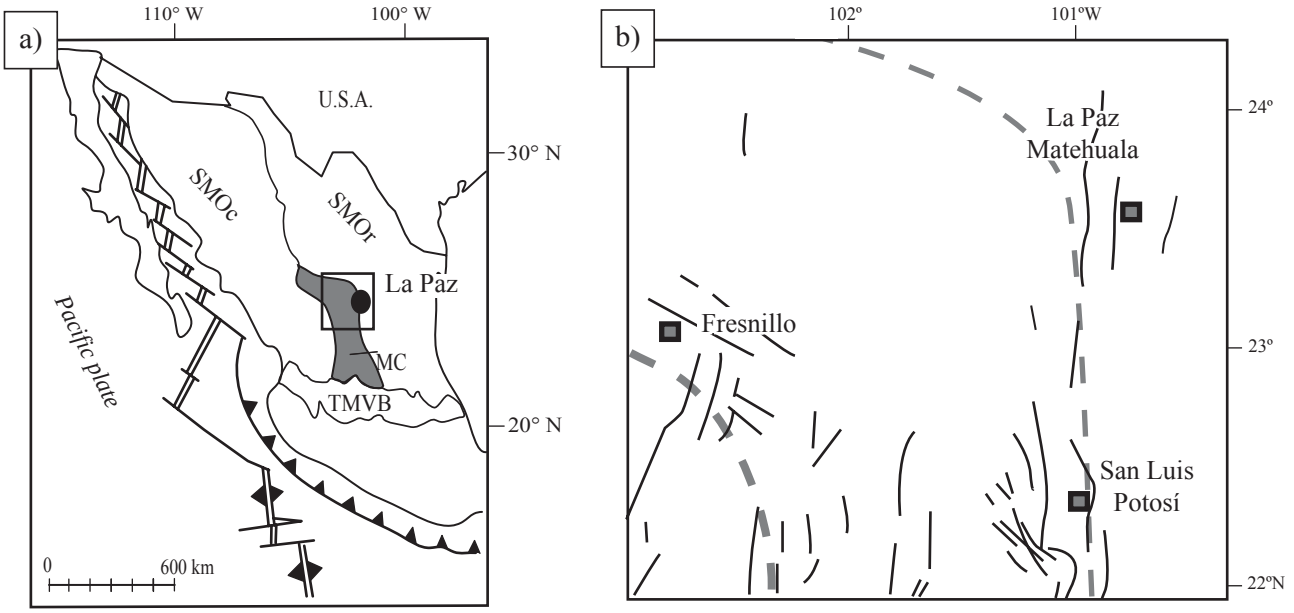


Figure 1. a: Physiographic map of central Mexico. MC: Mesa Central; SMOr: Sierra Madre Oriental; SMOc: Sierra Madre Occidental; TMVB: Trans-Mexican Volcanic Belt. b: Main structural features of the northeasthern Mesa Central; modified after Nieto-Samaniego *et al.* (2005).

Locally, very small alkaline basalt flows of Miocene to Quaternary age also appear. The Laramide orogeny affected all the Mesozoic sedimentary column and caused folding and reverse faulting of the whole sedimentary sequence. Locally, one of the mid-scale related structures, the Dolores fault (Figure 2), with an estimated vertical displacement of 500 to 1000 m controls the outcropping of the mineralized system (Spurr *et al.*, 1912). The basin of the La Paz district is covered by alluvial sediments with ages spanning from the Pleistocene to present.

In La Paz district, the oldest outcropping sediments are limestones and shales that belong to the Albian-Cenomanian Cuesta del Cura Formation, with up to 200 m in thickness (García-Gutiérrez, 1967; Machado, 1970; Barboza-Gudiño *et al.*, 2004). This unit is overlain by the Turonian-Coniacian Indidura Formation (locally also known as Agua Nueva Formation) composed by alternating limestones and shales (Barboza-Gudiño *et al.*, 2004). The Caracol Formation (locally known as San Felipe and Méndez formations), of Santonian-Maastrichtian age (Barboza-Gudiño *et al.*, 2004) is composed by alternating limestones and shales with up to 100 m thick. All this Cretaceous sedimentary column is crosscuted by a granodiorite intrusion, that developed a metasomatic aureole with an associated Au-Cu skarn mineralization.

An ENE-WSW branching fault system crosscuts the skarn, and acted as a channelway for both dyke emplacement and the formation of a hydrothermal vein system. The San Acacio and San Augustín dykes are spatially related to the Ag-Pb-Zn-bearing vein system (Castro-Larragoitia, 1990). These veins display a mineralogical zonation, from Cu-Ag-Pb-Zn-Au-bearing veins near the intrusive stocks to Ag-Pb-Zn-Cu-bearing veins enclosed within either dykes or limestones, and to Ag-Pb-Zn-rich veins exclusively enclosed in limestones, the latter representing the apical part of the vein system towards the east end of the mineralized structures (Figure 2). The N-S and E-W fault systems present a complex polyphase movement history, both pre and post mineralization (Gunnesch *et al.*, 1994).

## ANALYTICAL TECHNIQUES

### Zircon recovery

Four granodiorite samples, of approximately 50 kg each, were obtained from four different locations (Dolores, Cobriza, and Membrillo stocks and the San Acacio dyke; Figure 2) for zircon separation. The samples were crushed, powdered and sieved (200 to 50 mesh) prior to mineral separation. Mineral fractions were obtained by density preconcentration with the use of heavy liquids (bromoform and methylene iodide). The non-magnetic fraction was separated with a Cook isodynamic magnet. Final zircon mineral fractions were hand picked under a binocular microscope and mounted in epoxy resin together with a standard (91500; Wiedenbeck *et al.*, 1995), and subsequently polished and gold coated.

### U-Pb age dating

Zircons recovered from the La Paz intrusions were carefully selected for dating. The selected grains display

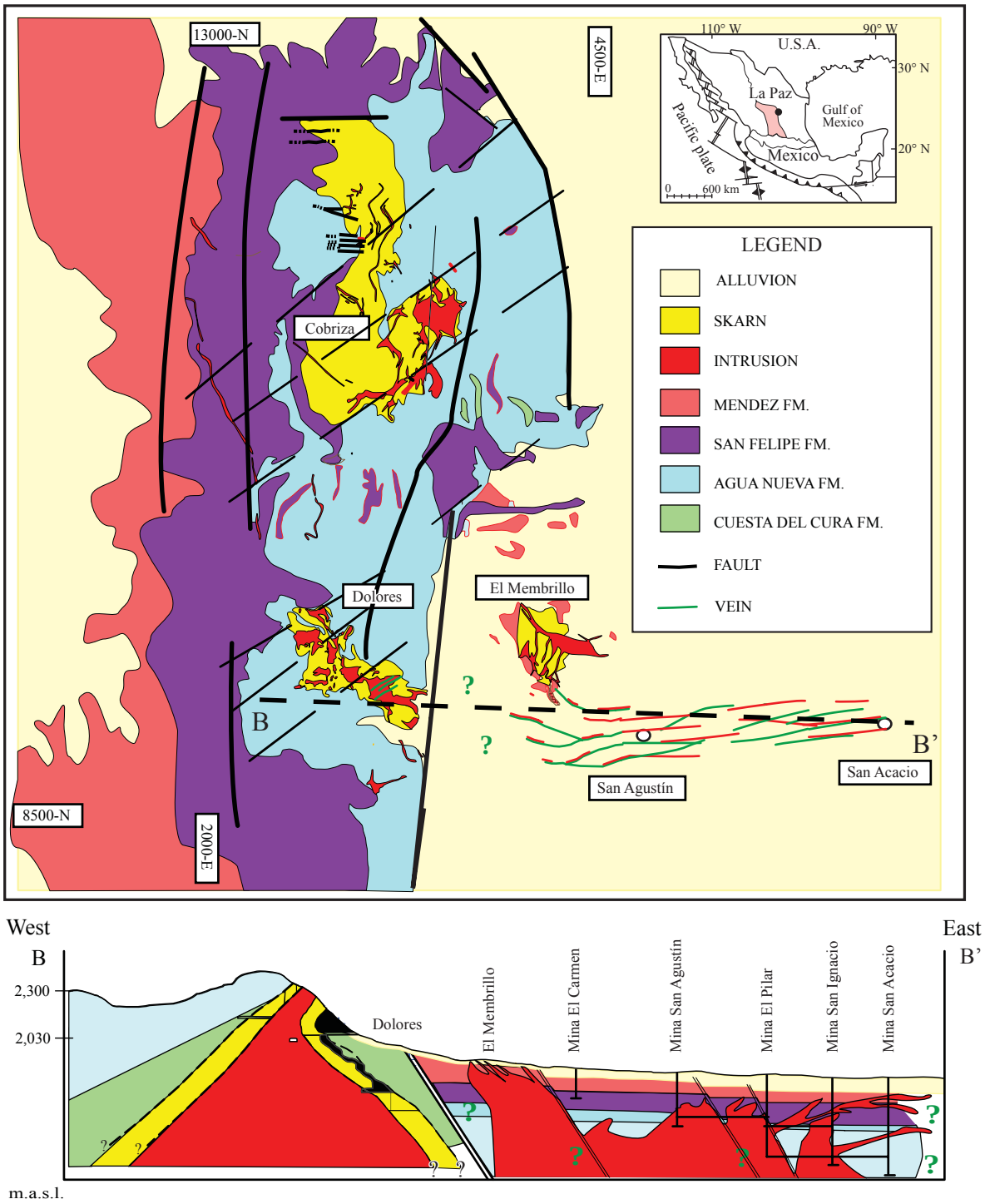


Figure 2. a: Geological map of the La Paz Au-Cu district. b: E-W cross section of the southern part of the La Paz Au-Cu district.

well-preserved prismatic shapes and euhedral growth zones, suggesting that they are of magmatic origin (Pupin, 1992), and no significant subsequent resorption and/or recrystallization.

Analyses were carried out at the University of Arizona (V.A. Valencia, analyst) with a LA-ICPMS Micromass system (Dickinson and Gehrels, 2003). 50–35 micron spots were analyzed with an output energy of ~32 mJ and a repetition rate of 10 Hz. Each analysis consisted on a background measurement (20 second integrations on peaks with no laser firing) and twenty second integrations on peaks with the laser firing on. Any $^{204}$Hg contribution to the $^{204}$Pb mass is accordingly removed by subtracting the background values. The collectors were configured for simultaneous measure-

ment of $^{204}Pb$ in an ion-counting channel and $^{206}Pb$, $^{207}Pb$, $^{208}Pb$, $^{232}Th$, and $^{238}U$ in Faraday detectors. All analyses were conducted in static mode. Inter-element fractionation was monitored using a standard (SL-1, natural zircon, 564±4 Ma; G.E. Gehrels, unpublished data). The reported ages for zircon grains are based entirely on $^{206}Pb/^{238}U$ ratios because errors of the $^{207}Pb/^{235}U$ and $^{206}Pb/^{207}Pb$ ratios are significantly greater. This is due primarily to the low intensity (commonly <0.5 meV) of the $^{207}Pb$ signal from these young, low-U grains. $^{207}Pb/^{235}U$ and $^{206}Pb/^{207}Pb$ ratios and ages are accordingly not reported. The $^{206}Pb/^{238}U$ ratios were corrected for common Pb by using the measured $^{206}Pb/^{204}Pb$, a common Pb composition from Stacey and Kramers (1975), and an uncertainty of 1.0 on the common $^{206}Pb/^{204}Pb$. The weighted mean of ~20 individual analyses was calculated according to Ludwig (2003) for each sample. This measurement error is added quadratically to the systematic errors, which include contributions from the calibration correction, decay constant, age of the calibration standard, and composition of common Pb. The systematic errors are 1–2% for these samples. Isotopic ratios and ages are reported in Table 1.

### Geochemical analyses

Rock samples were analyzed for major and trace elements at the SARM of the CRPG-CNRS (Nancy France). Whole-rock samples were crushed and powdered in an agate mortar and pestle, and divided into two equivalent portions. For major and trace element analyses, sample powders (300 mg) were decomposed by fusion with lithium metaborate and subsequently diluted using a HCl solution.

Major elements analyses were performed with a Jobin-Yvon JY70 Inductively Coupled Plasma-Atomic Emission Spectrometer (ICP-AES). Analytical precision was estimated at ±0.2% for $SiO_2$, and ±1% for the other major elements. The relative deviations of the standard analyses to the reference values are typically well below 1%.

Trace elements were analyzed with a Perkin Elmer ELAN 5000 Inductively Coupled Plasma-Mass Spectrometrer (ICP-MS). The analytical procedure was validated by repeated independent sample preparation, blanks, and analysis of international reference standards. The relative deviations of the standard analyses to the reference values are typically below 1%. Major and trace-element analysis are reported in Tables 2 and 3.

### Petrography

Mineralization and alteration relationships were examined by field and underground reconnaissance mapping, optical petrography and electron microprobe analyses. Mineral phases and compositions were determined with a Cameca SX 100 electron microprobe (voltage: 15 kV; intensity: 10 nA; raster length, 25 micron) at the University of Nancy, France.

## RESULTS

Four principal stocks and a dyke trend are recognized within the district crosscutting the whole sedimentary sequence. The horst and graben configuration controls the outcropping structural level. So, at the horst, the granodiorite stocks with associated Cu-Au skarn mineralization outcrop in Cobriza and Dolores; at the graben, part of the former stock as well as some blind dykes can be found in the underground mining works, including the western Au-Cu mineralizing stocks (El Membrillo and San Agustín mines) and, in the eastern part, the Ag-Pb-Zn vein mine of San Acacio (Figure 2).

### Petrography

The studied stocks present an overall porphyritic texture, where the phenocrysts are essentially composed by zoned plagioclase (oligoclase– andesine; 35–40%), K-feldspar (orthoclase-microcline, 30–25%), quartz (20–25%), and mafic minerals (biotite, hornblende, 8–10%), with accessory zircon, apatite and titanite, all included in a groundmass composed by quartz and feldspar microliths (Figure 3). As a local observation, the size of the phenocrysts progressively diminishes from Dolores to Cobriza (south to north), and from Dolores to Membrillo and San Agustín (west to east). The San Acacio dykes present a clear porphyritic texture, with phenocrysts of millimetric size. The phenocrysts are mainly composed by zoned plagioclase (andesine; 32–50%), quartz (30%), K-feldspar (orthoclase-microcline, 15%), and rare mafic minerals (biotite, hornblende, 5%), with accessory zircon, apatite and titanite, all included in a groundmass composed by quartz and feldspar microlits.

The metasomatism caused by the intrusion of the granodioritic stocks, as well as by some dykes (San Acacio dyke excluded), is marked by the presence of the mineralized skarn itself affecting the Mesozoic carbonates, and of heavily recrystallized rocks, locally classified as "hornfels", affecting the more argillaceous sedimentary materials (San Felipe and Méndez formations). The size and form of the metasomatic and metamorphic aureoles are directly related to the arrangement of the main anisotropies affecting the Mesozoic sediments (estratification joints, type and intensity of fracturation, folding, etc.) as well as to their chemical composition. The hornfels present granoblastic textures with garnet, wollastonite and diopside as main minerals.

As a general rule within the disctrict, the endoskarn rarely attain more than 1 m in thickness when is fully developed, being composed mainly by grossular-rich garnet and diopside, with minor vesuvianite and accessory titanite. The exoskarn is always very well developed, with a variable

Table 1. U/Pb isotopic data for single zircon crystal from La Paz intrusives obtained by LA-ICPMS.

| Sample | U (ppm) | Th (ppm) | U/Th | $^{206}Pb/^{204}Pb_c$ | $^{207}Pb/^{235}U$ ratio | ± (%) | $^{206}Pb/^{238}U$ ratio | ± (%) | err corr | $^{206}Pb/^{207}Pb$ ratio | ± (%) | $^{206}Pb/^{238}U$ Age (Ma) | ± (Ma) | $^{207}Pb/^{235}U$ Age (Ma) | ± (Ma) | $^{206}Pb/^{207}Pb$ Age (Ma) | ± (Ma) |
|---|---|---|---|---|---|---|---|---|---|---|---|---|---|---|---|---|---|
| *Horst - stock* | | | | | | | | | | | | | | | | | |
| Dolores zirc. 1 | 546 | 174 | 3.1 | 263 | | | 0.00585 | 3.32 | | | | 37.6 | 1.2 | | | | |
| Dolores zirc. 2 | 246 | 75 | 3.3 | 123 | | | 0.00582 | 6.55 | | | | 37.4 | 2.4 | | | | |
| Dolores zirc. 3 | 95 | 69 | 1.4 | 128 | | | 0.00581 | 8.88 | | | | 37.4 | 3.3 | | | | |
| Dolores zirc. 4 | 752 | 104 | 7.2 | 360 | | | 0.00569 | 1.82 | | | | 36.6 | 0.7 | | | | |
| Dolores zirc. 5 | 758 | 99 | 7.7 | 485 | | | 0.00565 | 2.06 | | | | 36.3 | 0.7 | | | | |
| Dolores zirc. 6 | 1234 | 187 | 6.6 | 1014 | | | 0.00580 | 2.19 | | | | 37.3 | 0.8 | | | | |
| Dolores zirc. 7 | 707 | 119 | 6.0 | 375 | | | 0.00571 | 2.72 | | | | 36.7 | 1.0 | | | | |
| Dolores zirc. 8 | 728 | 109 | 6.7 | 381 | | | 0.00568 | 2.08 | | | | 36.5 | 0.8 | | | | |
| Dolores zirc. 9 | 664 | 110 | 6.0 | 349 | | | 0.00562 | 3.78 | | | | 36.1 | 1.4 | | | | |
| Dolores zirc. 10 | 899 | 931 | 1.0 | 710 | | | 0.00559 | 1.63 | | | | 36.0 | 0.6 | | | | |
| Dolores zirc. 11 | 293 | 45 | 6.5 | 240 | | | 0.00574 | 3.89 | | | | 36.9 | 1.4 | | | | |
| Dolores zirc. 12 | 493 | 81 | 6.1 | 493 | | | 0.00570 | 2.44 | | | | 36.7 | 0.9 | | | | |
| Dolores zirc. 13 | 511 | 148 | 3.5 | 287 | | | 0.00572 | 3.02 | | | | 36.8 | 1.1 | | | | |
| Dolores zirc. 14 | 650 | 105 | 6.2 | 694 | | | 0.00581 | 2.60 | | | | 37.4 | 1.0 | | | | |
| Dolores zirc. 15 | 1692 | 1509 | 1.1 | 640 | | | 0.00572 | 1.48 | | | | 36.8 | 0.5 | | | | |
| Dolores zirc. 16 | 940 | 298 | 3.2 | 976 | | | 0.00570 | 3.33 | | | | 36.6 | 1.2 | | | | |
| Dolores zirc. 17 | 1091 | 193 | 5.7 | 746 | | | 0.00572 | 1.72 | | | | 37.6 | 0.6 | | | | |
| Dolores zirc. 18 | 760 | 170 | 4.5 | 635 | | | 0.00582 | 1.92 | | | | 37.4 | 0.7 | | | | |
| Dolores zirc. 19 | 750 | 151 | 5.0 | 323 | | | 0.00571 | 4.25 | | | | 36.7 | 1.6 | | | | |
| Dolores zirc. 20 | 468 | 279 | 1.7 | 482 | | | 0.00567 | 1.69 | | | | 36.4 | 0.6 | | | | |
| Dolores zirc. 21 | 193 | 57 | 3.4 | 1040 | 1.00385 | 5.27 | 0.10032 | 3.49 | 0.66 | 11,378 | 3.94 | 616.3 | 20.5 | 705.8 | 26.8 | 1,002 | 80 |
| Dolores zirc. 22 | 280 | 65 | 4.3 | 498 | 0.17645 | 10.73 | 0.02690 | 3.23 | 0.30 | 12,102 | 10.23 | 171.1 | 5.5 | 165.0 | 16.3 | 79 | 244 |
| Dolores zirc. 23 | 878 | 118 | 7.4 | 6696 | 0.59534 | 6.58 | 0.05887 | 5.95 | 0.90 | 11,363 | 2.82 | 368.8 | 21.3 | 474.3 | 25.0 | 1,023 | 57 |
| Dolores zirc. 24 | 616 | 129 | 4.8 | 810 | 0.04546 | 24.24 | 0.00885 | 9.18 | 0.38 | 12,465 | 22.44 | 56.8 | 5.2 | 45.1 | 10.7 | - | - |
| Cobriza zirc.1 | 433 | 85 | 5.1 | 537 | | | 0.00551 | 2.71 | | | | 35.4 | 1.0 | | | | |
| Cobriza zirc.2 | 245 | 125 | 2.0 | 455 | | | 0.00549 | 6.02 | | | | 35.3 | 2.1 | | | | |
| Cobriza zirc.3 | 596 | 606 | 1.0 | 2293 | | | 0.00565 | 2.29 | | | | 36.3 | 0.8 | | | | |
| Cobriza zirc.4 | 266 | 36 | 7.3 | 1099 | | | 0.00572 | 4.85 | | | | 36.8 | 1.8 | | | | |
| Cobriza zirc.5 | 244 | 38 | 6.4 | 429 | | | 0.00566 | 4.79 | | | | 36.4 | 1.7 | | | | |
| Cobriza zirc.6 | 220 | 21 | 10.7 | 307 | | | 0.00555 | 7.84 | | | | 35.7 | 2.8 | | | | |
| Cobriza zirc.7 | 146 | 48 | 3.0 | 358 | | | 0.00572 | 7.06 | | | | 36.7 | 2.6 | | | | |
| Cobriza zirc.8 | 238 | 71 | 3.4 | 288 | | | 0.00573 | 7.10 | | | | 36.9 | 2.6 | | | | |
| Cobriza zirc.9 | 407 | 88 | 4.6 | 818 | | | 0.00583 | 5.38 | | | | 37.5 | 2.0 | | | | |
| Cobriza zirc.10 | 396 | 83 | 4.8 | 739 | | | 0.00565 | 1.60 | | | | 36.3 | 0.6 | | | | |
| Cobriza zirc.11 | 574 | 161 | 3.6 | 2683 | | | 0.00583 | 7.49 | | | | 37.5 | 2.8 | | | | |
| Cobriza zirc.12 | 393 | 95 | 4.2 | 1390 | | | 0.00562 | 4.01 | | | | 36.1 | 1.4 | | | | |
| Cobriza zirc.13 | 334 | 99 | 3.4 | 1353 | | | 0.00575 | 5.33 | | | | 36.9 | 2.0 | | | | |
| Cobriza zirc.14 | 411 | 68 | 6.0 | 765 | | | 0.00552 | 3.54 | | | | 35.5 | 1.3 | | | | |
| Cobriza zirc.15 | 603 | 213 | 2.8 | 1488 | | | 0.00576 | 4.25 | | | | 37.0 | 1.6 | | | | |
| Cobriza zirc.16 | 366 | 79 | 4.6 | 668 | | | 0.00556 | 4.46 | | | | 35.7 | 1.6 | | | | |
| Cobriza zirc.17 | 665 | 191 | 3.5 | 1202 | | | 0.00555 | 1.66 | | | | 35.7 | 0.6 | | | | |
| Cobriza zirc.18 | 368 | 105 | 3.5 | 1401 | | | 0.00556 | 4.24 | | | | 35.7 | 1.5 | | | | |
| Cobriza zirc.19 | 423 | 114 | 3.7 | 1476 | | | 0.00557 | 2.70 | | | | 35.8 | 1.0 | | | | |
| Cobriza zirc.20 | 1322 | 192 | 6.9 | 3989 | | | 0.00552 | 4.23 | | | | 35.5 | 1.5 | | | | |
| Cobriza zirc.21 | 263 | 49 | 5.4 | 1574 | | | 0.01134 | 3.17 | | | | 72.7 | 2.3 | | | | |

Table 1 (continued). U/Pb isotopic data for single zircon crystal from La Paz intrusives obtained by LA-ICPMS.

| Sample | U (ppm) | Th (ppm) | U/Th | $^{206}Pb/^{204}Pb_c$ | $^{207}Pb/^{235}U$ ratio | ± (%) | $^{206}Pb/^{238}U$ ratio | ± (%) | err corr | $^{206}Pb/^{207}Pb$ ratio | ± (%) | $^{206}Pb/^{238}U$ Age (Ma) | ± (Ma) | $^{207}Pb/^{235}U$ Age (Ma) | ± (Ma) | $^{206}Pb/^{207}Pb$ Age (Ma) | ± (Ma) |
|---|---|---|---|---|---|---|---|---|---|---|---|---|---|---|---|---|---|
| *Graben - stock* | | | | | | | | | | | | | | | | | |
| Membrillo zirc.1 | 443 | 142 | 3.1 | 802 | | | 0.00564 | 2.11 | | | | 36.3 | 0.8 | | | | |
| Membrillo zirc.2 | 702 | 231 | 3.0 | 813 | | | 0.00572 | 2.31 | | | | 36.8 | 0.8 | | | | |
| Membrillo zirc.3 | 791 | 149 | 5.3 | 869 | | | 0.00572 | 2.35 | | | | 36.8 | 0.9 | | | | |
| Membrillo zirc.4 | 276 | 139 | 2.0 | 404 | | | 0.00567 | 3.23 | | | | 36.4 | 1.2 | | | | |
| Membrillo zirc.5 | 712 | 105 | 6.8 | 1379 | | | 0.00586 | 1.80 | | | | 37.7 | 0.7 | | | | |
| Membrillo zirc.6 | 547 | 93 | 5.9 | 428 | | | 0.00570 | 3.62 | | | | 36.6 | 1.3 | | | | |
| Membrillo zirc.7 | 159 | 94 | 1.7 | 279 | | | 0.00589 | 4.75 | | | | 37.8 | 1.8 | | | | |
| Membrillo zirc.8 | 456 | 76 | 6.0 | 862 | | | 0.00567 | 3.41 | | | | 36.5 | 1.2 | | | | |
| Membrillo zirc.9 | 392 | 84 | 4.7 | 1113 | | | 0.00585 | 4.41 | | | | 37.6 | 1.7 | | | | |
| Membrillo zirc.10 | 309 | 50 | 6.1 | 1238 | | | 0.00571 | 4.13 | | | | 36.7 | 1.5 | | | | |
| Membrillo zirc.11 | 337 | 294 | 1.1 | 883 | | | 0.00599 | 4.48 | | | | 38.5 | 1.7 | | | | |
| Membrillo zirc.12 | 469 | 115 | 4.1 | 995 | | | 0.00566 | 2.75 | | | | 36.4 | 1.0 | | | | |
| Membrillo zirc.13 | 621 | 196 | 3.2 | 229 | | | 0.00548 | 8.67 | | | | 35.2 | 3.0 | | | | |
| Membrillo zirc.14 | 728 | 229 | 3.2 | 2016 | | | 0.00573 | 2.20 | | | | 36.8 | 0.8 | | | | |
| Membrillo zirc.15 | 212 | 85 | 0.6 | 267 | | | 0.00575 | 3.04 | | | | 37.0 | 1.1 | | | | |
| Membrillo zirc.16 | 1185 | 2008 | 0.6 | 1947 | | | 0.00572 | 3.58 | | | | 36.8 | 1.3 | | | | |
| Membrillo zirc.17 | 171 | 104 | 1.6 | 296 | | | 0.00560 | 6.87 | | | | 36.0 | 2.5 | | | | |
| Membrillo zirc.18 | 572 | 183 | 3.1 | 2219 | | | 0.00589 | 3.09 | | | | 37.8 | 1.2 | | | | |
| Membrillo zirc.19 | 466 | 303 | 1.5 | 1359 | | | 0.00562 | 2.63 | | | | 36.1 | 0.9 | | | | |
| Membrillo zirc.20 | 362 | 90 | 4.0 | 1074 | | | 0.00595 | 6.44 | | | | 38.2 | 2.5 | | | | |
| Membrillo zirc.21 | 97 | 28 | 3.4 | 621 | | | 0.00585 | 5.76 | | | | 37.6 | 2.2 | | | | |
| Membrillo zirc.22 | 738 | 312 | 2.4 | 2482 | | | 0.00582 | 1.94 | | | | 37.4 | 0.7 | | | | |
| Membrillo zirc.23 | 694 | 425 | 1.6 | 21575 | 1.25566 | 4.08 | 0.12018 | 3.68 | 0.90 | 13,196 | 1.77 | 731.6 | 25.5 | 826.0 | 23.1 | 1,089 | 35 |
| Membrillo zirc.24 | 451 | 132 | 3.4 | 2690 | 0.15286 | 8.23 | 0.01767 | 4.02 | 0.49 | 15,941 | 7.18 | 112.9 | 4.5 | 144.4 | 11.1 | 699 | 153 |
| Membrillo zirc.25 | 219 | 153 | 1.4 | 320 | 0.18531 | 24.18 | 0.02674 | 2.95 | 0.12 | 19,892 | 24.00 | 170.1 | 5.0 | 172.6 | 38.4 | 207 | 564 |
| *Graben - Dyke* | | | | | | | | | | | | | | | | | |
| San Acacio zirc. 1 | 1092 | 216 | 5.1 | 1253 | | | 0.00547 | 1.34 | | | | 35.1 | 0.5 | | | | |
| San Acacio zirc. 2 | 503 | 85 | 5.9 | 386 | | | 0.00548 | 2.52 | | | | 35.2 | 0.9 | | | | |
| San Acacio zirc. 3 | 423 | 72 | 5.8 | 211 | | | 0.00549 | 2.72 | | | | 34.4 | 0.9 | | | | |
| San Acacio zirc. 4 | 298 | 72 | 4.1 | 134 | | | 0.00564 | 8.77 | | | | 36.2 | 3.2 | | | | |
| San Acacio zirc. 5 | 70 | 28 | 2.5 | 88 | | | 0.00560 | 11.48 | | | | 36.0 | 4.1 | | | | |
| San Acacio zirc. 6 | 520 | 148 | 3.5 | 300 | | | 0.00547 | 3.52 | | | | 35.1 | 1.2 | | | | |
| San Acacio zirc. 7 | 269 | 37 | 7.2 | 171 | | | 0.00566 | 4.69 | | | | 36.4 | 1.7 | | | | |
| San Acacio zirc. 8 | 950 | 169 | 5.6 | 740 | | | 0.00536 | 1.85 | | | | 34.5 | 0.6 | | | | |
| San Acacio zirc. 9 | 888 | 170 | 5.2 | 941 | | | 0.00532 | 2.39 | | | | 34.2 | 0.8 | | | | |
| San Acacio zirc. 10 | 769 | 253 | 3.0 | 338 | | | 0.00553 | 2.65 | | | | 35.6 | 0.9 | | | | |
| San Acacio zirc. 11 | 504 | 52 | 9.7 | 363 | | | 0.00558 | 2.77 | | | | 35.9 | 1.0 | | | | |
| San Acacio zirc. 12 | 583 | 9 | 63.5 | 551 | | | 0.00559 | 2.58 | | | | 35.9 | 0.9 | | | | |
| San Acacio zirc. 13 | 884 | 348 | 2.5 | 156 | | | 0.00513 | 9.81 | | | | 33.0 | 3.2 | | | | |
| San Acacio zirc. 14 | 640 | 116 | 5.5 | 294 | | | 0.00536 | 3.29 | | | | 34.5 | 1.1 | | | | |
| San Acacio zirc. 15 | 639 | 146 | 4.4 | 162 | | | 0.00539 | 6.73 | | | | 34.6 | 2.3 | | | | |
| San Acacio zirc. 16 | 1039 | 174 | 6.0 | 897 | | | 0.00530 | 2.39 | | | | 34.1 | 0.8 | | | | |
| San Acacio zirc. 17 | 490 | 240 | 2.0 | 211 | | | 0.00545 | 3.70 | | | | 35.0 | 1.3 | | | | |
| San Acacio zirc. 18 | 555 | 318 | 1.7 | 266 | | | 0.00548 | 3.54 | | | | 35.3 | 1.2 | | | | |
| San Acacio zirc. 19 | 433 | 79 | 5.5 | 280 | | | 0.00545 | 3.94 | | | | 35.2 | 1.4 | | | | |
| San Acacio zirc. 20 | 860 | 171 | 5.0 | 374 | | | 0.00547 | 2.32 | | | | 35.2 | 0.8 | | | | |
| San Acacio zirc. 21 | 493 | 101 | 4.9 | 4643 | 0.49252 | 4.83 | 0.06140 | 3.81 | 0.79 | 17.188 | 2.97 | 384.1 | 14.2 | 406.6 | 16.2 | 537 | 65 |
| San Acacio zirc. 22 | 220 | 55 | 4.0 | 1260 | 0.27599 | 12.75 | 0.03849 | 6.38 | 0.50 | 19,230 | 11.04 | 243.5 | 15.2 | 247.5 | 28.0 | 285 | 253 |

Table 2. Major and trace-element analyses of the intrusives from la Paz Au-Cu Skarn deposits. < L.D.: below the detection limit.

| | **Graben - dyke** | **Graben - stock** | | **Horst - stock** | | | |
|---|---|---|---|---|---|---|---|
| | **San Acacio** | **San Agustín** | **Membrillo** | **Cobriza-1** | **Cobriza-2** | **Dolores-1** | **Dolores-2** |
| Size ($km^2$) | 0.01 | 0.15 | 0.35 | 1.9 | 1.9 | 0.8 | 0.8 |
| *Oxides (wt.%)* | | | | | | | |
| $SiO_2$ | 61.58 | 61.27 | 62.91 | 68.24 | 67.97 | 66.49 | 66.35 |
| $TiO_2$ | 0.66 | 0.89 | 0.84 | 0.56 | 0.62 | 0.62 | 0.6 |
| $Al_2O_3$ | 15.25 | 16.48 | 16.24 | 14.89 | 14.76 | 15.72 | 16.16 |
| $Fe_2O_3$ | 3.82 | 2.84 | 4.74 | 3.42 | 3.3 | 2.62 | 3.38 |
| MnO | 0.12 | 0.03 | 0.04 | 0.05 | 0.03 | 0 | 0 |
| MgO | 0.94 | 1.31 | 1.73 | 0.78 | 0.81 | 1.11 | 0.73 |
| CaO | 4.22 | 6.6 | 5.4 | 3.98 | 4.75 | 4.84 | 3.98 |
| $Na_2O$ | 2.07 | 2.8 | 3.05 | 3.03 | 2.9 | 2.82 | 2.94 |
| $K_2O$ | 6.7 | 5.3 | 3.72 | 4.36 | 4.01 | 4.4 | 4.17 |
| $P_2O_5$ | 0.22 | 0.26 | 0.28 | 0.27 | 0.24 | 0.23 | 0.23 |
| **LOI** | 5.13 | 3.02 | 1.77 | 0.79 | 0.52 | 1.06 | 1.31 |
| Total | 100.7 | 100.77 | 100.71 | 100.37 | 99.91 | 99.91 | 99.85 |
| *Trace elements (ppm)* | | | | | | | |
| Be | 2 | 1.7 | 2 | 2.5 | 2.2 | 2.3 | 2.4 |
| V | 55.7 | 75.2 | 55.7 | 24.1 | 31.6 | 44.7 | 46.2 |
| Cr | 6.3 | 5.6 | 5.3 | 4.6 | 0 | 4.5 | 4.5 |
| Co | 6.2 | 5.6 | 4.9 | 3.9 | 4.3 | 3.4 | 5 |
| Ni | < L.D. | < L.D. | 4.1 | < L.D. | < L.D. | < L.D. | < L.D. |
| Cu | 5.8 | 539.9 | 38.9 | 25.5 | 21.3 | 209.4 | 109.4 |
| Zn | 50.9 | 102.9 | 58.3 | 69.9 | 75.9 | 182.3 | 37.3 |
| Ga | 22.2 | 23.4 | 21.6 | 21.7 | 20.7 | 20.7 | 23.1 |
| Ge | 1.3 | 1.4 | 1.8 | 1.6 | 1.5 | 1.6 | 1.6 |
| As | 33 | 665 | 4.3 | 1.7 | 1.3 | 6.9 | 14.6 |
| Rb | 335 | 205.1 | 139.6 | 128.8 | 96.3 | 119.5 | 145.7 |
| Sr | 248.5 | 594 | 662 | 503.9 | 662.9 | 457.8 | 461.7 |
| Y | 18 | 22.8 | 23.1 | 12.3 | 12.8 | 14 | 13 |
| Zr | 181.9 | 208.1 | 193.8 | 211.3 | 178.2 | 175.5 | 194.7 |
| Nb | 9.9 | 10.7 | 9.9 | 11.3 | 10.3 | 10 | 10.9 |
| Mo | 1.7 | 13.2 | 0.8 | 62 | 16.1 | 3 | 3.7 |
| Cd | < L.D. | 1.5 | 0.4 | 0.5 | 0.5 | 0.9 | < L.D. |
| In | 0.1 | 0.3 | 0.1 | 0.1 | 0.1 | 0.1 | < L.D. |
| Sn | 2.8 | 50 | 1 | 6.8 | 2.6 | 7.1 | 4.3 |
| Sb | 9.9 | 0.8 | 3.5 | < L.D. | < L.D. | 1.2 | 42.4 |
| Cs | 11.5 | 21 | 4.3 | 5.3 | 3.6 | 5.1 | 7.1 |
| Ba | 919.5 | 827.6 | 828.8 | 684.7 | 690.1 | 639.2 | 678.4 |
| La | 26.7 | 33.4 | 33.4 | 31.2 | 23.6 | 30.4 | 27.8 |
| Ce | 55.1 | 68 | 68.3 | 63.3 | 48.7 | 76.1 | 76.7 |
| Pr | 7.1 | 8.7 | 8.8 | 8.4 | 6.5 | 9.2 | 8.2 |
| Nd | 28.4 | 34.9 | 34.5 | 33.6 | 26.6 | 34.8 | 33.1 |
| Sm | 5.8 | 6.9 | 6.7 | 6.8 | 5.6 | 6.5 | 6.9 |
| Eu | 1.4 | 1.7 | 1.6 | 1.5 | 1.5 | 1.4 | 1.7 |
| Gd | 4.6 | 5.6 | 5.3 | 5 | 4.5 | 4.9 | 6.5 |
| Tb | 0.7 | 0.8 | 0.8 | 0.6 | 0.6 | 0.7 | 0.8 |
| Dy | 3.4 | 4.4 | 4.4 | 2.9 | 2.9 | 3.4 | 3.9 |
| Ho | 0.6 | 0.8 | 0.8 | 0.5 | 0.5 | 0.6 | 0.6 |
| Er | 1.6 | 2.1 | 2.2 | 1.4 | 1.5 | 1.5 | 1.6 |
| Tm | 0.2 | 1.9 | 0.3 | 0.2 | 0.2 | 0.2 | 0.2 |
| Yb | 1.5 | 1.9 | 2.1 | 1.3 | 1.2 | 1.3 | 1.4 |
| Lu | 0.2 | 0.3 | 0.3 | 0.2 | 0.2 | 0.2 | 0.2 |
| Hf | 4.8 | 5.5 | 5.2 | 5.5 | 4.8 | 4.7 | 5.4 |
| Ta | 1.1 | 1 | 1 | 1.2 | 1.1 | 1.1 | 1.2 |
| W | 1.8 | 5.5 | 3.1 | 2.5 | 4.9 | 7.7 | 3.2 |
| Pb | 20.5 | 9.5 | 22.3 | 10 | 11 | 8.3 | 8 |
| Bi | < L.D. | 1 | < L.D. | < L.D. | < L.D. | 4.7 | 0.4 |
| Th | 8.1 | 8.2 | 8.7 | 8.7 | 7 | 11.6 | 20.4 |
| U | 3.6 | 2.7 | 2.8 | 3.8 | 3.1 | 4 | 4.8 |
| Grade Cu (%) | 0.2 | 1.3 | 1 | 2 | 1.9 | 1.5 | 1 |
| Grade Au (g/t) | 0.02 | 0.1 | 0.08 | 0.6 | 0.5 | 1.5 | 1 |
| Eu/Eu* | 0.83 | 0.82 | 0.82 | 0.81 | 0.9 | 0.74 | 0.65 |
| Sm/Yb | 3.87 | 3.59 | 3.17 | 5.22 | 4.66 | 5 | 4.93 |
| La/Sm | 4.59 | 4.82 | 4.98 | 4.6 | 4.21 | 4.68 | 4.03 |

Table 3. Comparison table of the major and trace element composition of La Paz granitoids, with worldwide skarn-associated plutons (Meinert, 1995), and worldwide adakite (Martin *et al.*, 2005). D: dyke; I: Intrusive; mw: mining works; sup: superficial.

| | **Worldwide skarn** | | | **Worldwide adakite** | | **La Paz Au-Cu Skarn** | | | | | | |
|---|---|---|---|---|---|---|---|---|---|---|---|---|
| | Au skarns | Cu skarns | All skarns | Adakite HSA (n=267) | | San Acacio D | San Agustin I | Membrillo I | Cobriza I | Cobriza I | Dolores I | Dolores I |
| | Mean | Mean | Mean | Mean | SD | Graben-mw | Graben-mw | Graben-sup | Horst-sup | Horst- mw | Horst-sup | Horst- mw |
| $SiO_2$ | 61.4 | 64.90 | 66.80 | 64.80 | 2.5 | 61.58 | 61.27 | 62.91 | 68.24 | 67.97 | 66.49 | 66.35 |
| $TiO_2$ | 0.6 | 0.50 | 0.50 | 0.56 | 0.1 | 0.66 | 0.89 | 0.84 | 0.56 | 0.62 | 0.62 | 0.6 |
| $Al_2O_3$ | 16.2 | 16.00 | 15.10 | 16.64 | 0.9 | 15.25 | 16.48 | 16.24 | 14.89 | 14.76 | 15.72 | 16.16 |
| $Fe_2O_3$ | 2.6 | 2.50 | 1.90 | 4.75 | 1.0 | 3.82 | 2.84 | 4.74 | 3.42 | 3.3 | 2.62 | 3.38 |
| FeO | 3.7 | 2.40 | 2.50 | - | - | | | | | | | |
| MnO | 0.1 | 0.10 | 0.10 | 0.08 | 0.02 | 0.12 | 0.03 | 0.04 | 0.05 | 0.03 | 0 | 0 |
| CaO | 5.8 | 3.80 | 3.80 | 4.63 | 0.8 | 4.22 | 6.60 | 5.40 | 3.98 | 4.75 | 4.84 | 3.98 |
| MgO | 3.2 | 1.80 | 1.80 | 2.18 | 0.7 | 0.94 | 1.31 | 1.73 | 0.78 | 0.81 | 1.11 | 0.73 |
| $K_2O$ | 2.5 | 3.6 | 3.70 | 1.97 | 0.5 | 6.70 | 5.30 | 3.72 | 4.36 | 4.01 | 4.4 | 4.17 |
| $Na_2O$ | 3.1 | 4.00 | 3.50 | 4.19 | 0.4 | 2.07 | 2.80 | 3.05 | 3.03 | 2.9 | 2.82 | 2.94 |
| $P_2O_5$ | 0.2 | 0.30 | 0.20 | 0.2 | 0.2 | 0.22 | 0.26 | 0.28 | 0.27 | 0.24 | 0.23 | 0.23 |
| *Trace elements (ppm)* | | | | | | | | | | | | |
| V | 99 | 85 | 88 | 95 | 31 | 55.7 | 75.2 | 55.7 | 24.1 | 31.6 | 44.7 | 46.2 |
| Cr | 51 | 18 | 49 | 41 | 26 | 6.3 | 5.6 | 5.3 | 4.6 | 0.0 | 4.5 | 4.5 |
| Ni | 18 | 16 | 19 | 20 | 10 | - | - | 4.1 | - | - | - | - |
| Rb | 69 | 103 | 230 | 52 | 21 | 335.0 | 205.1 | 139.6 | 128.8 | 96.3 | 119.5 | 145.7 |
| Sr | 601 | 807 | 425 | 565 | 150 | 248.5 | 594.0 | 662.0 | 503.9 | 662.9 | 457.8 | 461.7 |
| Y | 17 | 17 | 39 | 10 | 3 | 18.0 | 22.8 | 23.1 | 12.3 | 12.8 | 14.0 | 13.0 |
| Zr | 116 | 183 | 131 | 108 | 41 | 181.9 | 208.1 | 193.8 | 211.3 | 178.2 | 175.5 | 194.7 |
| Nb | 9 | 9 | 18 | 6 | 2 | 9.9 | 10.7 | 9.9 | 11.3 | 10.3 | 10.0 | 10.9 |
| Ba | 891 | 1466 | 701 | 721 | 286 | 919 | 827 | 828 | 684 | 690 | 639 | 678 |
| La | 28 | 45 | 29 | 19.20 | 8 | 26.7 | 33.4 | 33.4 | 31.2 | 23.6 | 30.4 | 27.8 |
| Ce | 55 | 78 | 68 | 37.70 | 16 | 55.1 | 68.0 | 68.3 | 63.3 | 48.7 | 76.1 | 76.7 |
| Nd | 9 | 11 | 17.0 | 18.20 | 7 | 28.4 | 34.9 | 34.5 | 33.6 | 26.6 | 34.8 | 33.1 |
| Sm | - | - | - | 3.40 | 1.30 | 5.8 | 6.9 | 6.7 | 6.8 | 5.6 | 6.5 | 6.9 |
| Eu | - | - | - | 0.90 | 0.30 | 1.4 | 1.7 | 1.6 | 1.5 | 1.5 | 1.4 | 1.7 |
| Gd | - | - | - | 2.80 | 0.80 | 4.6 | 5.6 | 5.3 | 5.0 | 4.5 | 4.9 | 6.5 |
| Dy | - | - | - | 1.90 | 0.50 | 3.4 | 4.4 | 4.4 | 2.9 | 2.9 | 3.4 | 3.9 |
| Er | - | - | - | 0.96 | 0.30 | 1.6 | 2.1 | 2.2 | 1.4 | 1.5 | 1.5 | 1.6 |
| Yb | - | - | - | 0.88 | 0.20 | 1.5 | 1.9 | 2.1 | 1.3 | 1.2 | 1.3 | 1.4 |
| Lu | - | - | - | 0.17 | 0.04 | 0.2 | 0.3 | 0.3 | 0.2 | 0.2 | 0.2 | 0.2 |
| $K_2O/Na_2O$ | 0.80 | 0.9 | 1.05 | 0.47 | 1.25 | 3.24 | 1.89 | 1.22 | 1.42 | 1.38 | 1.56 | 1.42 |
| Sr/Y | 35.35 | 47.47 | 10.89 | 56 | 5.0 | 14 | 26 | 29.0 | 41.0 | 52 | 33 | 35 |

thickness between 10 and 100 m. The exoskarn presents five mineralogically well defined metasomatic zones: 1) hedenbergite-diopside-bearing inner zone, with minor andraditic-garnet at the intrusive contact (Figure 3); 2) andradite-diopside-bearing zone; 3) grossular-rich garnet-wollastonite-bearing zone away from the intrusive; 5) an outer, heavily recrystallized limestone zone ("marble") of variable thickness (10–20 m) that gradually passes to the non-recrystallized limestone.

A pervasive retrograde alteration affects both the endoskarn and exoskarn. This alteration phase is characterized by a penetrative stockwork structure composed by thin mineralized veinlets with associated propylitic alteration (actinolite, tremolite, chlorite, epidote, sericite, calcite and quartz) usually with sulfide minerals (mainly Ag-rich galena, sphalerite, chalcopyrite, pyrite, pyrargyrite, and tetrahedrite; Figure 3). Most of the gold present either in the endoskarn or exoskarn is associated with the retrograde veinlets. Also, the Dolores skarn presents a significant higher gold grade (>0.5 gr) than the Cobriza and Membrillo skarns.

## U-Pb dating

Twenty-five analyses performed on the Dolores granodiorite zircons provided $^{206}Pb/^{238}U$ ages dispersed between 36.0±0.6 Ma and 1,356.9±96 Ma. The weighted mean crystallizing age of these zircons was calculated according to Ludwig (2003) as 36.8±0.5 Ma (n=20; MSWD of 1.4; see Figure 4 and Table 1). We also found two other concordant ages that revealed the existence of two older magmatic events of respectively Paleocene (57±5 Ma, n=1) and Bathonian (171±6 Ma, n=1) ages. Three other discordant ages exhibit inherited Mesoproterozoic ($^{206}Pb/^{207}Pb$: *ca.* 1,000 Ma, upper intersect; n=2) and Paleoproterozoic ages ($^{206}Pb/^{207}Pb$: 1,890±57 Ma, n=1).

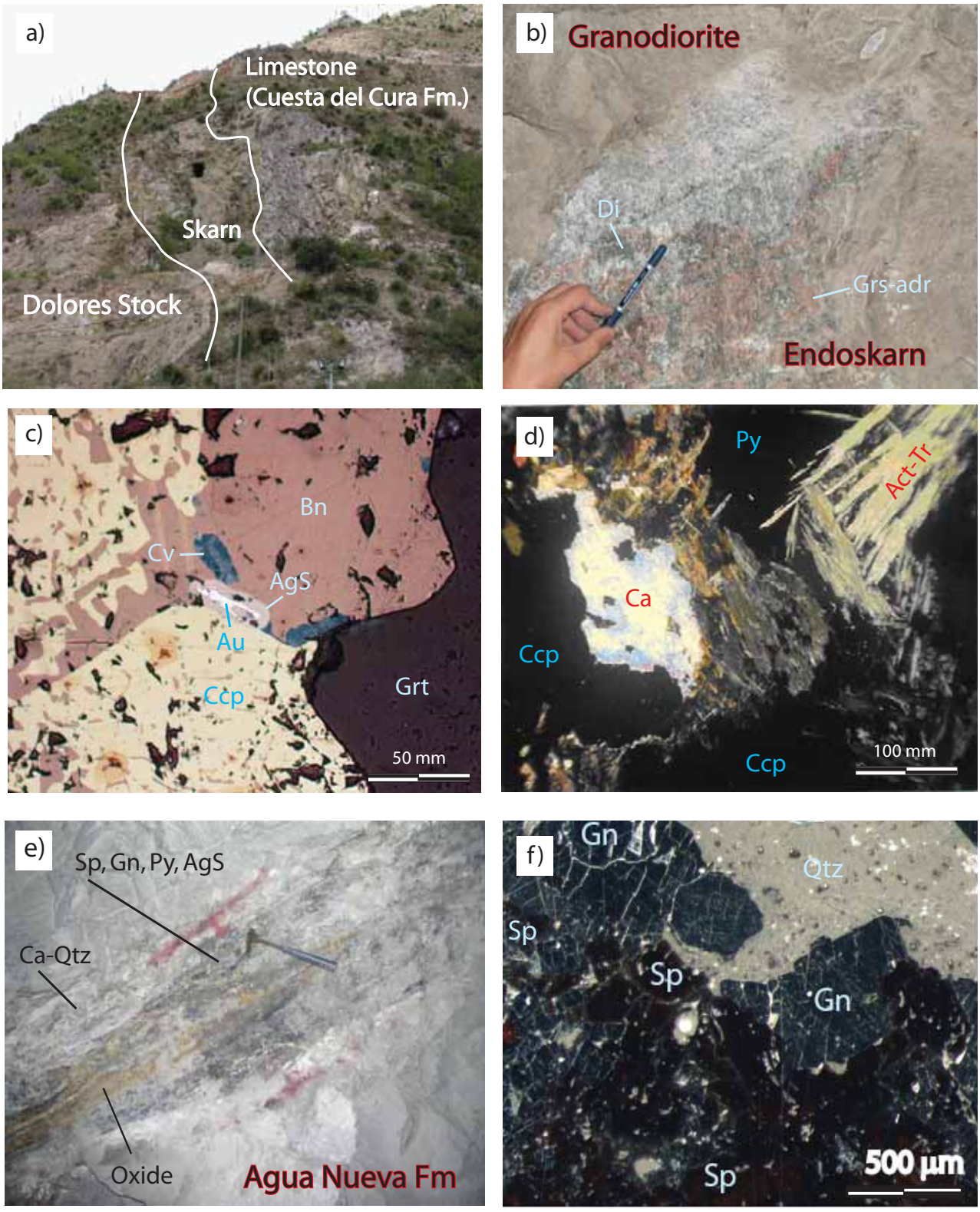


Figure 3. a: Panoramic view of the Dolores Skarn outcrop; b: Contact between the Granodiorite intrusive and the endoskarn at Cobriza mine; c: Microphotography of prograde mineralization from Cobriza exoskarn mine; Chalcopyrite-bornite interdigitation. d: microphotography of the retrograde mineralization in the Dolores exoskarn; calcite and actinolite-tremolite cementing the mineralization. e: El Pilar vein, 1550 m level. Silver, galena and sphalerite mineralization associated to quartz gangue. The vein crosscut a granodiorite stock. f: microphotography of the El Pilar galena-sphalerite vein mineralization. Abbreviation used; Act: Actinolite; Adr: andradite; AgS: silver sulphide; Au: gold; Bn: bornite; Ca: calcite; Ccp: chalcopyrite; Cv: covelite; Di: diopside; Gn: galena, Grs: grossular; Grt: Garnet; Py: pyrite; Qtz: quartz; Sp: sphalerite; Tr: Tremolite.

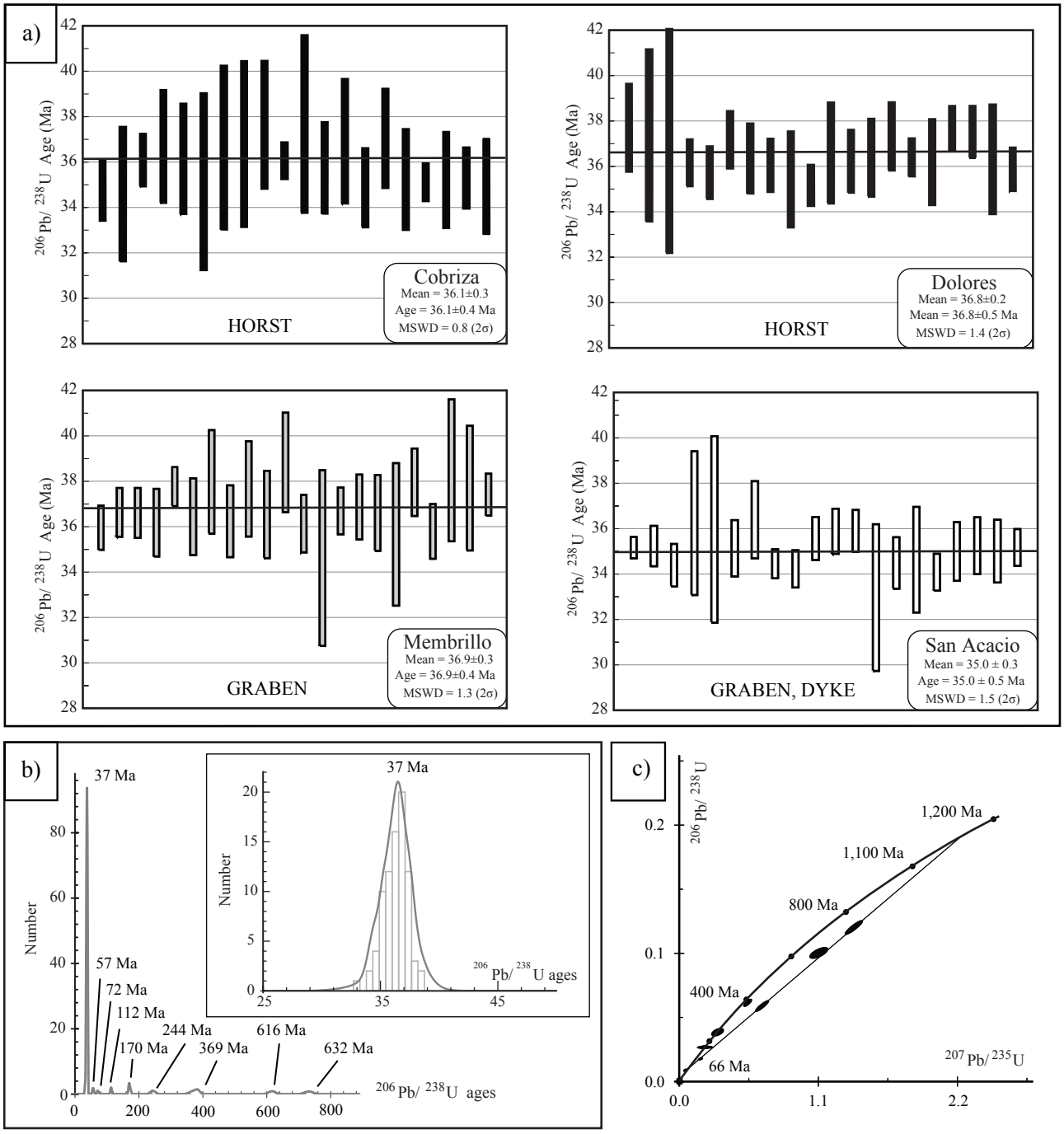


Figure 4. a: $^{206}Pb/^{238}U$ zircon ages of the La Paz intrusives obtained by LA-ICPMS. b: Statistical distribution of the $^{206}Pb/^{238}U$ zircon ages of all analyzed intrusives of the La Paz district (calculated with the Isoplot program; Ludwig 2003). c: $^{206}Pb/^{238}U$ versus $^{207}Pb/^{235}U$ plot for the LA-ICPMS zircon analyses. Ages, means and mean standard weighted deviation (MSWD) were calculated with the Isoplot program (Ludwig, 2003). Errors are given in 2σ. See text for further discussion.

Twenty-one analyses performed in the Cobriza intrusive zircons indicated $^{206}Pb/^{238}U$ ages dispersed between 35.3±2.1 Ma and 37.5±2.8 Ma. The weighted mean crystallizing age for these zircons is calculated, according to Ludwig (2003), as 36.1±0.4 Ma (n=20; MSWD of 0.8; Figure 4 and Table 1). One concordant age suggested the existence of an older magmatic event of Maastrichtian age (72±5 Ma, n=1).

For the El Membrillo intrusive, twenty-five analyses provided $^{206}Pb/^{238}U$ ages comprised between 35.2±3.0 Ma and 731.6±25.5 Ma. The weighted mean crystallizing age of zircons is calculated according to Ludwig (2003) at

36.9±0.4 Ma. (n=22; MSWD of 1.3; Figure 4 and Table 1). Three other discordant ages suggest the existence of three older magmatic events of namely Jurassic ($^{206}Pb/^{207}Pb$: *ca.* 200, n=1), Neoproterozoic ($^{206}Pb/^{207}Pb$: *ca.* 700 Ma, n=1), and Mesoproterozoic ($^{206}Pb/^{207}Pb$: *ca.* 1,000 Ma, upper intercept, n=1) ages.

For the San Acacio dykes, twenty-two analyses provided $^{206}Pb/^{238}U$ ages dispersed between 33.0±3.2 Ma and 384±14 Ma. The weighted mean crystallizing age of zircons from the San Acacio granodiorite dykes, according to Ludwig (2003) is 35.0±0.5 Ma (n=20; MSWD of 1.5; Figure 4, Table 1). Two older magmatic events were also revealed with Permian ($^{206}Pb/^{207}Pb$: *ca.* 285 Ma, n=1) and Cambrian ($^{206}Pb/^{207}Pb$: *ca.* 537 Ma, n=1) ages.

All the weighted mean crystallizing ages found are considered as representative of the emplacement ages of the intrusives. These newly found ages are in concordance with the data obtained by Tuta *et al.* (1988) (*ca.* 36 Ma, K-Ar in biotite from the Dolores intrusive)

## Major and trace elements behaviour

At La Paz, the sampled granitoids present a small compositions variation in major and trace elements (see Table 2). As the samples were taken from both the graben and horst mining works and surface, these minor geochemical differences can be explained as representing different structural levels of the same intrusive. Samples of the La Paz Au-Cu skarn have variable loss on ignition (LOI; 0.52 to 5.13%; Table 2) reflecting variable $H_2O$ contents, possibly due to different degrees of alteration. In general, the high-field-strength elements (HFSE) and rare earth elements (REE), are essentially immobile during intense hydrothermal alteration (Hawkesworth *et al.*, 1997). The major elements contents (except $Na_2O$ and $K_2O$) of La Paz intrusive show no obvious correlation with increasing LOI, indicating that their contents have probably not been changed by alteration. All rock types show mostly metaluminous ($61\% < SiO_2 < 68\%$), high-K calc-alkaline affinities ($4\% < K_2O < 7\%$); they belong either to a high-K calc-alkaline magmatic series (Le Maitre *et al.*, 1989), or to the alkali-calcic metaluminous (Frost *et al.*, 2001) series (Figure 5). Chondrite-normalized REE patterns (Figure 6) show that all samples are enriched in light REE (LREE) with respect to the heavy REE (HREE). They are moderately fractionated [$11.64 < (La/Yb)_N < 15.2$] with relatively low $Yb_N$ contents (≤10), small negative Eu anomalies ($0.65 < Eu/Eu^* < 0.9$), and high REE contents (ΣREE up to1,800 ppm).

## DISCUSSION

The scattered mean statistic ages found for the studied stocks and dykes can have a dual interpretation. On one hand, it can be due to the presence of several magmatic pulses from the Membrillo stock 36.9±0,4 Ma to the San Acacio dyke 35±0.5 Ma (Figure 4, Table 1); on the other hand, considering the short standard variation of the general statistic distribution, it can be an artefact caused by sampling at different vertical levels, obtaining slightly different samples within a narrow variability range. This last explanation have the authors preference

The late Eocene age of La Paz intrusives (*ca.* 37 Ma) is contemporaneous with the Mapimi Cu-Zn skarn deposit (Durango; 36 Ma, K-Ar in plagioclase; Megaw *et al.*, 1988) and the Ag-Pb-Zn skarn-vein system of Fresnillo (32 Ma, K-Ar in plagioclase; Lang *et al.*, 1988; Simmons, 1991). They represent the latests episodes of the syn/post-orogenic magmatism and related mineralizations in the Sierra de Catorce district, that span from the Ag-Pb-Zn-Au veins at Real de Catorce (53±4 Ma, K-Ar in plagioclase, Mújica-Mondragón and Jacobo-Albarrán, 1983) to the Zn-Cu skarn at Charcas (43±3 Ma, K-Ar in orthoclase; Mújica-Mondragón and Jacobo-Albarrán, 1963).

Four of the discordant analyses constitute an isochrone, with the lower intersection close to 60 Ma and the upper at around 1,100 Ma. Therefore, the upper intersection probably corresponds to Mesoproterozoic inherited zircon grains, that were incorporated into the granodioritic magma during its formation or ascent through triassic sandstone and shale series (Silva-Romo, 1996; Silva-Romo *et al.*, 2000). This Grenvillian age is in agreement with the presence of old lower crust in the Mesa Central as shown by Schaaf *et al.* (1994), who obtained a Sm/Nd isochron age of 1,248±69 Ma for lower crustal xenoliths included in Quaternary volcanics of the Santo Domingo and Ventura maars (San Luis Potosí state, Mexico). Schaaf *et al.* (1994) interpreted this age as the intrusion age of a magmatic precursor. Moreover, calculated Nd crustal residence ages ($T_{DM}$) of the Oligocene volcanic sequence yield estimates of Precambrian age (980 to 1,000 Ma; Orozco-Esquivel, personal communication).

The general tendency, in terms of major elements, for the plutonic rocks associated to different types of skarn is towards calc-alkaline compositions (Fe, Au, Cu, Zn–Pb, W,

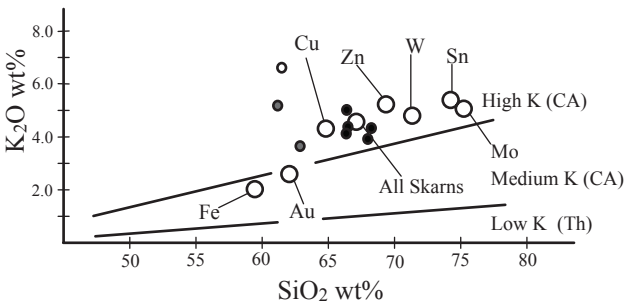


Figure 5. $K_2O$ *vs.* $SiO_2$ Harker diagram. Fields represent calc-alkaline (CA) and tholeitic (Th) affinities of plutons of the La Paz (black dot: horst; grey dot: graben; open dot: San Acacio dyke), open circles indicate the average values for different ore deposits reported by Meinert (1995).

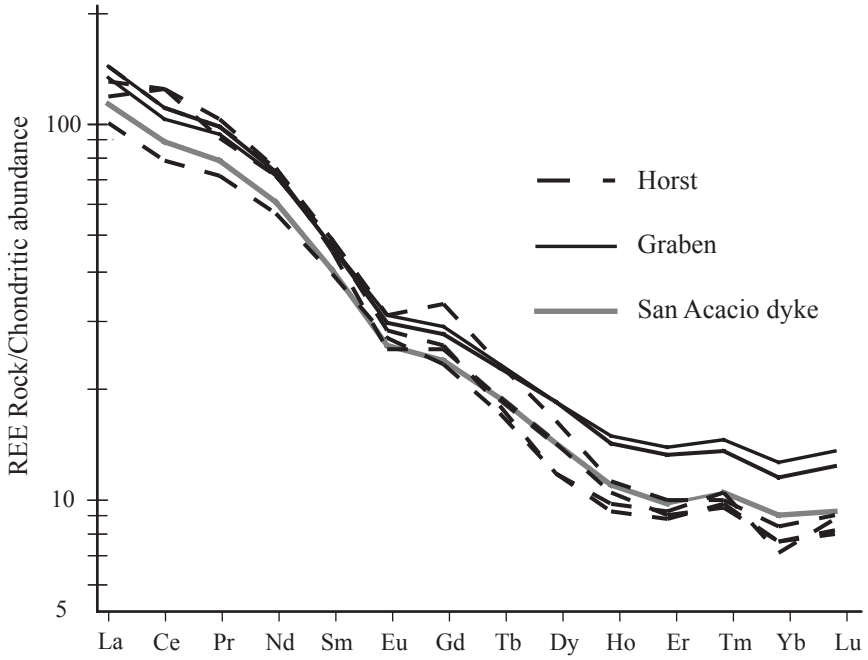


Figure 6. Chondrite normalized REE patterns for La Paz plutons. See explanation in the text.

Sn and Mo-bearing skarns; Figure 5; Meinert, 1995). All samples from La Paz granitoids correspond to high-K calc-alkaline rocks; the horst samples are tightly concentrated within the Cu and Zn rich skarns fields, whereas the graben granitoid samples and the San Acacio dyke plot scattered close to the Cu-rich skarns field. This scattering can reflect a hydrothermal influence on the original chemistry of the intrusives.

Table 3 presents a comparison among the chemical data from La Paz granitoids and other Au-related and Cu-related intrusive bodies abroad (Meinert, 1995), as well as high-$SiO_2$ (HSA) adakite rocks (Martin and Moyen, 2003; Martin *et al.*, 2005). The analyses of the major and trace elements reported by Meinert (1995) indicate that the plutonic rocks associated with Cu anomalies present a similar trend as the one shown by type I magmas. With the exception of the low $Na_2O$ contents, the La Paz western intrusives (Dolores and Cobriza) display certain geochemical affinity with HSA major and trace element, following the criteria defined by Defant and Drummond (1990), Drummond and Defant (1990), Drummond *et al.* (1996) and Martin (1999). At La Paz, the higher Sr values (467 to 653 ppm) shown by the granitoids, in contrast with the low Sr values found in the San Acacio dyke (248 ppm), are comparable with the values obtained for the giant porphyry copper deposits in the Andes (Reich *et al.*, 2003).

Figure 7 shows the relationship between mobile *vs.* inmobile elements. The Rb/Sr ratio is very sensitive to magmatic differentiation, and usually the Sn-, Mo-, and W-rich skarn magmas are highly differentiated with respect to Fe-, Au- and Cu-rich skarn-related magmas. In our case, the La Paz analyses show the same general tendency displayed by the Cu-rich skarn deposits. Our samples present high Zr concentrations, ranging from 176 to 211 ppm, with a low magmatic differentiation grade. Notably, the San Acacio dyke is more differentiated and present a similar tendency as the Zn deposits. In the La/Yb *vs.* Yb diagram (Figure 8), the samples of La Paz intrusives are consistent with a partial melting trend, indicating that their compositional variation is mainly controlled by this process rather than by fractional crystallization. However, the presence of inherited zircon grains and the large Mg-number [$100\times Mg^{2+}/(Mg^{2+}+Fe^{total})$] variation from 17 to 23 indicate that these magmas could

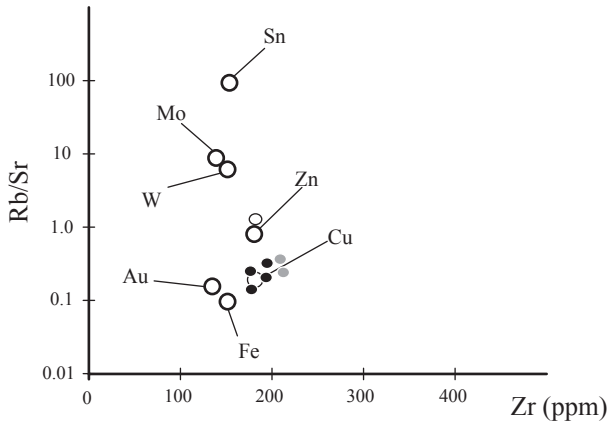


Figure 7. Trace element content of La Paz samples showed in a Rb/Sr *vs.* Zr plot; black dot: horst; grey dot: graben; open dot: San Acacio dyke. Open circles indicate the average values for different ore deposits reported by Meinert (1995).

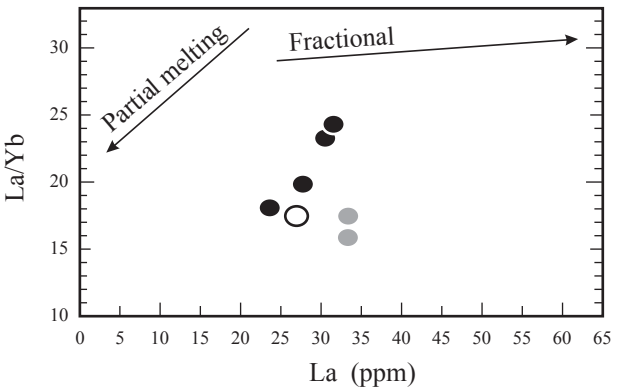


Figure 8. La/Yb *vs.* La diagram for the La Paz samples. Black dot: horst; grey dot: graben; open dot: San Acacio dyke.

be generated from metabasaltic magmas (Castillo *et al.*, 1999).

It is generally believed that reaction between pure slab melts and surrounding peridotite in the sub-arc mantle wedge results in the high Mg-number and MgO contents typical of adakites (see Figure 9a reference). In the Figure 9a, the La Paz samples mimetize the fields of "thick lower crust-derived adakite rock" and "metabasalt and eclogite experimental melts".

Figure 9b shows the $(La/Yb)_N$ *vs.* $Yb_N$ relationships. The samples from the graben stocks clearly overlap the field of "island arc" compositions, whereas the samples from the horst stocks fall within the "subducted oceanic crust derived adakites" field and span towards the field of "delaminated lower crust derived adakitic rocks", with low to moderate $(La/Yb)_N$ ratios. In La Paz samples, Y contents span from 12.3 to 14 ppm, with an average composition of 13 ppm, whereas Yb spans from 1.2 to 1.4, with an average content of 1.3 ppm. In contrast, well constrained adakites present compositions of Y< 18 ppm and Yb < 1.8 ppm, and typical calc-alkaline lavas have compositions of Yb>2.5 ppm and Y>25 ppm. Consequently, we can conclude that our intrusive probably represent a transition between these two compositional fields. The Sm/Yb ratios are used to calculate relative crustal thicknesses (Hildreth and Moorbath, 1988; Kay and Kay, 1991; Kay *et al.,* 1999). The increase in the Sm/Yb ratio reflects the pressure-dependent changes that occur in the transition from clinopyroxene to amphibole and, then, to garnet in the refractary residue that is in equilibrium with an evolving magma (Kay and Kay, 1991). So, clinopyroxene is dominant at depths less than 35 km, amphibole is stable between ~30 to 45 km, whereas garnet appears at depths greater than 45–50 km.

Figure 10 shows the La/Sm *vs.* Sm/Yb ratios for the La Paz granitoids as well as the compositional fields reported by Kay and Mpodozis (2001) for the porphyry copper ore deposits of El Teniente (Chile), and the Au-rich belt of El Indio (Chile). The intrusives related with the Au-Cu mineralization at La Paz present crustal La/Sm and Sm/Yb compositions comparable to those of the Andean region (30 to 45 km). These conclusions are in agreement with the occurrence of Oligocene granulite facies metamorphism at the base of the crust (Hayob *et al.*, 1989, Rudnick and Cameron, 1991) documented in granulite xenoliths included in Quaternary volcanics.

Major and trace elements display an evolution from low differentiated granodiorite magmas (horst) to the more differentiated shallowest magmatic bodies (San Acacio dyke). This continuum magmatic evolution supports the vertical geochemical variation already discussed above (U-Pb dating results and interpretation), rather than several magmatic pulses.

## Source of the La Paz intrusions

Under subduction settings, constrained by particular P-T-$H_2O$ conditions (P>5 kbar, TºC > 750ºC, >10 wt% $H_2O$), young (<25 Ma), mafic oceanic lithosphere melts before reaching dehydration, generating the "typical" adakitic magmas with a MORB-like isotopic signature, instead of the typical calc-alkaline arc andesite-dacite-rhyolite suites, originated by partial melting of a metasomatized mantle wedge (Drummond *et al.*, 1996; Martin, 1999; Prouteau *et al.*, 1999). However, adakite rocks have been found in various geological settings and their formation explained by several genetic models: 1) partial melting of a subducted oceanic crust slab (*e.g.*, Defant and Drumond, 1990; Martin *et al.*, 2005); 2) crustal assimilation and fractional crystallization processes (*e.g.*, Castillo *et al.*, 1999); 3) partial melting of a lower thickened crust (Kay *et al.*, 1978, 1991; Petford and Atherton 1996; Kay and Mpodozis, 2001; Atherton and Petford, 1993; Xiong *et al.*, 2003); 4) partial melting of a stalled slab in the mantle (*e.g.*, Mungall, 2002); and 5) partial melting of a delaminated lower crust (*e.g.*, Kay and Mahlburg-Kay, 1993; Wang *et al.*, 2004). On the basis of the local and regional tectonic settings at La Paz and Mesa Central respectively, as well as of the geochemical characteristics and the zircon U-Pb ages, the last two models (4 and 5) are more plausible than the first three other models to explain the generation of the La Paz fertile granodiorites.

The Laramide Orogeny in western Mexico was the consequence of low-angle, high-speed (14 cm/year) convergence and subduction processes between the Farallon and the North America plates, which occurred from the Maastrichtian to the Paleocene (Dickinson and Snyder, 1978; Clark *et al.*, 1982; Bird, 1988; Meschede *et al.*, 1997; Bunge and Grand, 2000). The Oligocene trench is supposed to have been in a geographic position comparable to the present subduction trench, at around 500 km from La Paz district (Schmid *et al.*, 2002). It is generally accepted that the Eocene-Oligocene magmatic activity in the Sierra Madre Occidental and the Mesa Central was still related to the sudbuction of the Farallon plate under North America

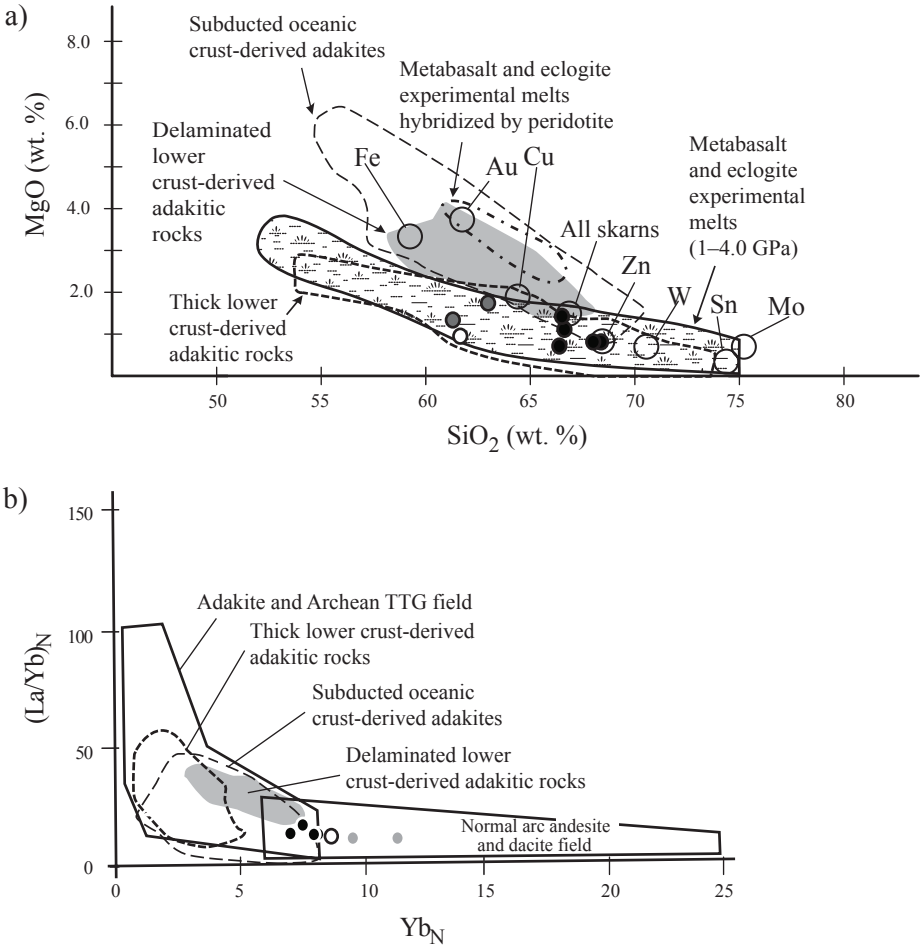


Figure 9. a: Harker MgO *vs.* $SiO_2$ diagram. Black dot: horst; grey dot: graben; open dot: San Acacio dyke. Open circles indicate the average values for different ore deposits reported by Meinert (1995). The field of metabasalt and eclogite experimental melts (1–4.0 GPa) is from Rapp *et al.* (1991, 1999, 2002), Sen and Dunn (1994), Rapp and Watson (1995), Prouteau *et al.* (1999), Skjerlie and Patiño Douce (2002), and references therein. The field of metabasalt and eclogite experimental melts hybridized with peridotite is after Rapp *et al.* (1999). The field of subducted oceanic crust-derived adakites is constructed using data from Defant and Drummond (1990), Kay and Mahlburg-Kay (1993), Drummond *et al.* (1996), Stern and Kilian (1996), Sajona *et al.* (2000), Aguillón-Robles *et al.* (2001), Defant *et al.* (2002), Calmus *et al.* (2003), Martin *et al.* (2005), and references therein. Data for thick lower crust-derived adakitic rocks are from Atherton and Petford (1993), Muir *et al.* (1995), Petford and Atherton (1996), Johnson *et al.* (1997), Xiong *et al.* (2003). b: $(La/Yb)_N$ *vs.* $Yb_N$ plot illustrating the field of adakites and calc-alkaline rocks. The La Paz intrusive rocks samples are symbolized as black dots: horst; grey dots: graben; open dots: San Acacio dyke. Data sources are the same than for Figure 9a.

(Dickenson and Snyder, 1978; Clark *et al.*, 1982; Bird, 1988; Meschede *et al.*, 1997; Bunge and Grand, 2000). Internal deformation of the Farallon slab in the transition zone is proposed to explain the inland extension of contemporary magmatism activity (Schmid *et al.*, 2002).

The orogen build-up was followed by two periods of post-orogenic extension illustrated by the appeareance of two volcanic events . The age of these volcanic sequences varies from 37 to 49 Ma and from 29 to 27 Ma (Labarthe-Hernández *et al.*, 1989; Ferrari *et al.*, 2005), respectively. The first event is interpreted as related to post-orogenic extension and the second one as a modification of the subduction direction (Ferrari *et al.*, 2005). Recently, Orozco-Esquivel *et al.* (2002) distinguished within the second volcanic event two sub-units, one classically related to mantle-derived magmas, and a second related to lower crust (of supposed Grenvillian age) partial melting with low mantle contributions. This second volcanic sub-unit is comparable in age and chemistry with the La Paz mineralized intrusives. The same authors suggested that the well-documented early Oligocene crustal extension in the Mesa Central (Nieto-Samaniego *et al.*, 1999) allowed basaltic melts to invade the crust, which subsequently acted as heat source for crustal melting. The granulite facies metamorphism would be then associated with this heating event and a crustal melting process that generated the upper, younger sequence of rhyolites. Melting occurred at high rates, causing a rapid increase in pore fluid pressure that reduced rock strength and promoted rock fracturing. Then, such conditions enhanced rock permeability and rapid melt segregation at low degrees of melting before equilibrium was attained (Petford, 1995; Knesel and Davidson, 1999). The

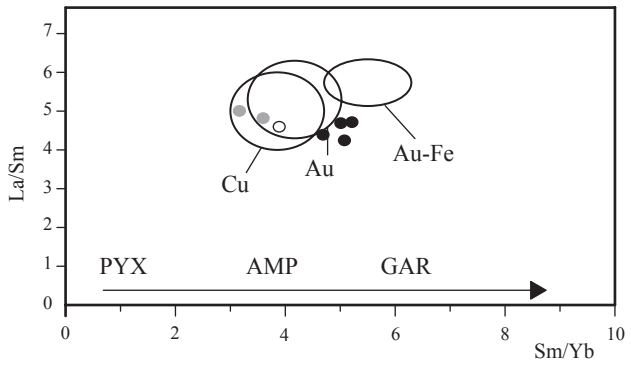


Figure 10. La/Sm *vs.* Sm/Yb plot showing the fields for the La Paz intrusives and those from the Au-rich belt El Indio and the Cu region El Teniente. With increasing the Sm/Yb ratio there is an increase of crustal thickness and pressure. PYX: pyroxene, AMP: amphibole, GAR: garnet (modified from Kay and Mpodozis, 2001). The La Paz samples are identified as: black dots: horst; grey dots: graben; open dots: San Acacio dyke.

same effect of enhanced permeability would be produced by the dehydration and melting of granulites under water-undersaturated conditions (Rushmer, 1996). Another factor promoting rapid melt segregation and ascent is a low melt viscosity (McKenzie, 1984). High crustal extension rates, as occurred at this time in the Mesa Central, would also helped rapid magma ascent to the upper crustal emplacement level. The conditions of a short-lived event of melt generation in an extensional stress field associated to rapid heating of source rocks, high melting rates, and fast melt segregation, support the possibility of generating magmas with anomalous adakite-like affinities.

### Source of metals

There has been a growing interest in adakitic magmatism and its relationship with copper and gold mineralization during the last decade. The physical association between adakites and ore deposits has been documented mainly in Philippines (Sillitoe and Gappe 1984; Malihan 1987; Imai *et al.,* 1993); the Chilean Andes (Thieblemont *et al.,* 1997) and in Mexico (González-Partida *et al.*, 2003). Porphyry copper and skarn deposits are generally derived from sulfur rich, highly oxidized magmatic system (Sillitoe, 1997; Oyarzun *et al.*, 2001; Mungall, 2002; Richards, 2002; Rabbia *et al.*, 2002). Mungall (2002) highlighted the importance of the $fO_2$ ( $fO_2$ > FMQ buffer) of the magma as limiting condition for the transport of chalcophile elements. Thieblemont *et al.* (1997), Mungall (2002), and Defant *et al.* (2002) identified slab-derived adakite magmas as the most favorable for Cu-Au mineralization, because of their high oxidizing potencial. The tectonic scenarios considered favorable for the generation of Cu-Ag magmatic mineralization after slab melting are subduction of a very young lithosphere, flat subduction, oblique convergence, and the presence of stalled slabs (Sillitoe, 1997; Mungall, 2002; Wang *et al.*, 2006).

Wang *et al.* (2006) proposed, besides $fO_2$ conditions, the generation of fertile adakite magmas by partial melting of a thick lower crust that interacted with the most important chalcophile reservoir, the mantle, in a geodynamic scenario without slab subduction. So, because the adakitic signatures are not exclusively generated by slab melting and can also been explained by crustal involvement, either as a magma contaminant or as a protholith after crustal thickening (Petford and Atherton, 1996; Kay and Mpodozis, 2001; Xu *et al.*, 2002; Zang *et al.*, 2005; Wang *et al.* 2006), a combination of geochemical and geodynamic evidences are needed to better constrain the adakite origin.

Paleotectonic reconstructions of the Mesa Central and geochemical evidences previously discussed from La Paz igneous rocks suggest that source magma could have been formed under garnet-amphibolite facies. It is noteworthy that the fluid release after breakdown of an amphibole-bearing mineralogy, passing to garnet-bearing residual assemblages during the melting process, has been considered of fundamental importance for the formation of the large central Andean ore deposits (Kay *et al.,* 1999; Kay and Mpodozis 2001, Wang *et al.*, 2006). As the chalcophile elements are mainly stored in mantle sulfides (Mungall, 2002), their transport from the mantle by magmas will only occur if the sulfide phases are completely consumed during partial melting under mantle oxidation conditions above the FMQ buffer (Mungall, 2002).

## CONCLUSIONS

The intrusive rocks intimately related with the La Paz Au-Cu skarn deposits display a transitional geochemical signature between the adakite and calc-alkaline compositions. The La Paz stocks were emplaced during the late Eocene crustal extension (*ca.* 37 Ma) that occurred after the Laramide Orogeny. Deep seated fault systems, as the Taxco-San Miguel de Allende fault system, channelled up and transported substantial quantities of heat and metal-bearing fluids to the upper lithosphere, favoring the formation of ore deposits. The extensional setting played a crucial role in the generation of adakite-like magmas by a combined process of lower crust delamination and partial melting (Figure 11).

## ACKNOWLEDGEMENTS

Our deep thankfulness to Lic. José Cerrillo Chowell, General Director of Negociación Minera Santa María de La Paz y Anexas, S.A. de C.V. for the support received for the fulfillment of the present study, and for allowing its publication. This study was financed by UNAM-PAPIIT projects IN114106 and IN100707, and CONACyT project 49234-F. We sincerely thank Professor Yang Xiaoyong, and Dr. Alaniz Álvarez for their constructive reviews.

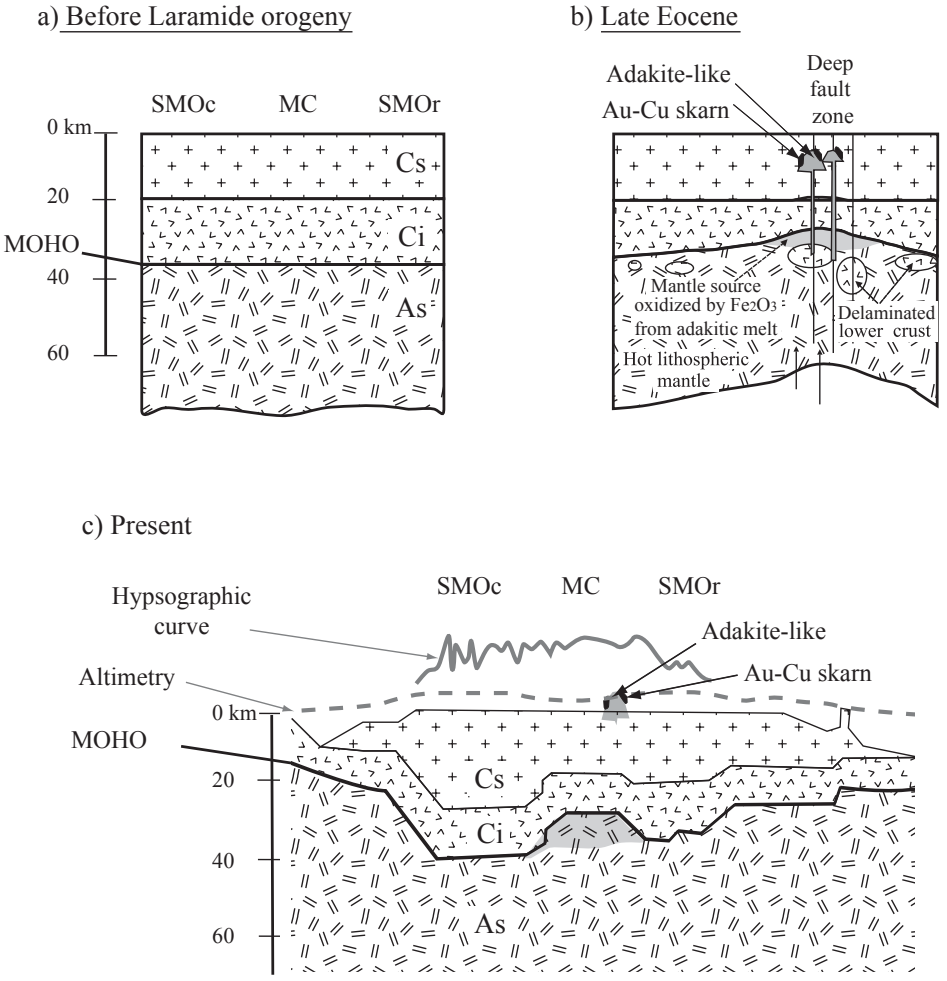


Figure 11. Suggested model to produce the La Paz adakite-like Au-Cu skarn via partial melting of delaminated lower crust in the late Eocene. a: The cold lithosphere and thick crust before the Laramide orogeny. The lower portion of the thick crust is composed of amphibole-bearing rocks. b: The hot asthenospheric mantle upwells in response to post-orogenic extension in the late Eocene (Nieto-Samaniego *et al.*, 2005); at the same time, fragments of the thick lower crust are removed through delamination. The delaminated lower crust begins to partially melt when it sinks into the underlying mantle. The adakitic melts are produced by partial melting of delaminated lower crust, which is heated by the surrounding relatively hot mantle, coupled with the flux of heat from the upwelling asthenosphere. The adakitic melts react with the surrounding mantle peridotite, elevating their MgO, Cr and Ni contents but reducing their FeO/MgO ratios. At the same time, the $fO_2$ of the surrounding mantle may have become elevated. The metallic sulfides in the mantle are oxidized, which causes the chalcophile elements to enter the adakitic magma. The generated magmas rise along a deep fault zone (*e.g.*, the Taxco-San Miguel de Allende deep fault zone). c: Present: accompanying lower crust delamination, surface erosion, and lithospheric or crustal extension result in the present-day thinned crust. Modified from Kerdan (1992) and Nieto-Samaniego *et al.* (2005).

## REFERENCES


Aguillón-Robles, A., Calmus, T., Bellon, H., Maury, R. C., Cotton, J., Bourgois, J., Michaud, F., 2001, Late Miocene adakites and Nb-enriched basalts from Vizcaino Peninsula, Mexico: indicators of East Pacific Rise subduction below southern Baja California: Geology, 29, 531–534.

Albinson, T., Nelson, C.E., 2001, New Mines and Discoveries in Mexico and Central America: Economic Special Publication 8, 362 p.

Atherton, M.P., Petford, N., 1993, Generation of sodium-rich magmas from newly underplated basaltic crust: Nature, 362, 144-146.

Barboza-Gudiño, J.R., Hoppe, M., Gómez-Anguiano, M., Martínez-Macias, P.R., 2004, Aportaciones para la interpretación estratigráfica y estructural de la porción noroccidental de la Sierra de Catorce, San Luis Potosí, Mexico: Revista Mexicana de Ciencias Geológicas, 21, 3, 299-320.

Bird, P.,1988, Formation of the Rocky Mountains, western United States: A continuum computer model: Science 239, 1501-1507.

Bunge, H.P., Grand, S.P., 2000, Mesozoic plate-motion history below the northeast Pacific Ocean from seismic images of the subducted Farallon slab: Nature, 18, 405, 337-340.

Calmus, T., Aguillon Robles, A., Maury, R.C., Bellon, H., Benoit, M., Cotton, J., Bourgois, J., Michaud, F., 2003, Spatial and temporal evolution of basalts and magnesian andesites(«bajaites») from Baja California, Mexico: the role of slab melts: Lithos, 66(1-2), 77-105.

Campa, M.F., Coney, P.J., 1984, Tectono-stratigraphic terranes and mineral resource distributions in Mexico: Canadian Journal of Earth Sciences, 20, 1040-1051.

Camus, F., 2003, Geología de los sistemas porfíricos en los Andes de Chile: Santiago, Chile, Servicio Nacional de Geología y Minería, 267 p.

Castillo, P.R., Janney, P.E., Solidum, R.U., 1999, Petrology and geochemistry of Camiguin island, southern Philippines: insights to the source of adakites and other lavas in a complex arc setting: Contributions to Mineralogy and Petrology, 134, 33–51.

Castro-Larragoitia, G.J., 1990, Investigaciones petrográficas y geoquímicas en el yacimiento de Ag-Pb-Zn-Cu de Santa María de La Paz, Matehuala, México: Alemania, Universidad de Karlsruhe, Instituto de Petrografía y Geoquímica, Diplom Thesis.

Cathles, L.M.,1981, Fluid flow and genesis of hydrothermal ore deposits, *in* Skinner B.J. (ed.), 75th anniversary volume: Economic Geology, 424-457.

Clark, A.H., 1993, Are outsize porphyry copper deposits either anatomically or environmentally distinctive?, *in* Whiting, B.H., Hodgson, C.J., Mason, R. (eds.), Giant ore deposits: Society of Economic Geologists, Special Publication 2, 213-283.

Clark, K.F., Foster,C.T., Damon,P.E., 1982, Cenozoic mineral deposits and subduction-related magmatic arcs in Mexico: Geological Society of America Bulletin, 93, 533-544.

Defant, M.J., Drummond, M.S., 1990, Derivation of some modern arc magmas by melting of young subducted lithosphere: Nature, 347, 662-665.

Defant M. J., Xu J. F., Kepezhinskas, P., Wang, Q., Zhang, Q., Xiao, L., 2002, Adakites: some variations on a theme: Acta Petrologica Sinica 18, 129–142.

Dickinson, W.R., Gehrels, G.E., 2003, U-Pb ages of detrital zircons from Permian and Jurassic eolian sandstones of the Colorado Plateau, USA: paleogeographic implications: Sedimentology and Geology, 163, 29-66.

Dickinson, W.R., Snyder, W.S., 1978, Plate tectonics of the Laramide Orogeny: Geological Society of America, Memoir 151, 355–366.

Drummond, M.S., Defant, M.J.,1990, A model for trondhjemite-tonalite-dacite genesis and crustal growth via slab melting: Journal Geophysical Research, 95, 21503-21521.

Drummond, M.S., Defant,M.J., Kepezhinkas,P.K., 1996, The petrogenesis of slab derived trondhjemite-tonalite-dacite/adakite magmas: Transaction of the Royal Society of Edinburgh, Earth Sciences, 87, 205-216.

Ferrari, L., Valencia-Moreno, M., Bryan, S., 2005, Magmatismo y tectónica en la Sierra Madre Occidental y su relación con la evolución de la margen occidental de Norteamérica: Boletín de la Sociedad Geológica Mexicana, 57(3), 343-378.

Frost, B.R., Barnes, C.G., Collins, W.J., Arculus, R.J., Ellis, D.J., Frost, C.D., 2001, Ageochemical classification for granitic rocks: Journal of Petrology, 42, 2033-2048.

García-Gutiérrez, C., 1967, Geología y paragénesis del distrito minero de Matehuala, San Luis Potosí, México: Boletín de la Sociedad Geológica Mexicana, 30, 29-62.

González-Partida, E., Levresse, G., Carrillo-Chávez, A., Cheilletz, A., Gasquet, D., Jones, D., 2003., Paleocene adakite Au-Fe bearing rocks, Mezcala, Mexico: evidence from geochemical characteristics: Journal of Geochemical Exploration, 80, 25-40.

Gunnesch, K.A., Torres-del Angel, C., Cuba-Castro, C., Saenz, J., 1994, The Cu-Au Skarn and Ag-Pb-Zn vein deposits of La Paz, northeastern Mexico: Mineralogical, paragenetic and fluid inclusion characteristics: Economic Geology, 98, 455-489.

Hayob, J.L., Essene, E.J., Ruiz, J., Ortega-Gutiérrez, F., Aranda-Gómez, J.J., 1989, Young high-temperature granulites from the base of the crust in central Mexico: Nature, 342, 265-268.

Hawkesworth, J.C., Turner, S.P., McDermot, F., Peate, D.W., Van Galsteren, P., 1997, U-Th isotopes in arc magmas: implications for elements transfer from the subducted crust: Science, 273, 551-555.

Hildreth, W., Moorbath, S., 1988, Crustal contributions to arc magmatism in the Andes of Central Chile: Contributions to Mineralogy and Petrology, 98, 455-489.

Imai, A.,Listanco, E.L., Fujii, T., 1993, Petrologic and sulfur isotopic significance of highly oxidized and sulfur-rich magma of Mt. Pinatubo, Philippines: Geology, 22, 699-702.

Johnson, K., Barnes, C.G., Miller, C.A., 1997, Petrology, geochemistry, and genesis of high-Al tonalite and trondhjemites of the Cornucopia stock, Blue Mountains, Northeastern Oregon: Journal of Petrology 38, 1585–1611.

Kay, R.W., Kay, S.M., 1991, Creation and destruction of lower continental crust: Geologische Rundschau, 80, 259-278.

Kay, R.W., Mahlburg-Kay, S., 1993, Delamination and delamination magmatism: Tectonophysics, 219(1-3), 177-189.

Kay, S.M., Mpodozis, C., 2001, Central Andean ore deposits linked to evolving shallow subduction system and thickening crust: GSA Today, 11, 4-9.

Kay, S.M., Mpodozis, C., Coira, B., 1999, Magmatism, tectonism, and mineral deposits of the Central Andes (22º-33º S), *in* Skinner, B. (ed.), Geology and Ore deposits of the Central Andes: Society of Economic Geology, Special Publication 7, 27-59.

Kerdan, T.P., 1992, Estructura de la corteza y manto superior en el norte de México (a lo largo del Trópico de Cáncer desde Baja California hasta el Golfo de México): México, Universidad Nacional Autónoma de México, Colegio de Ciencias y Humanidades, Unidad Académica de los Ciclos Profesionales y de Posgrado, M. Sc. Thesis, 347 p.

Knesel, K.M., Davidson, J.P., 1999, Sr isotope systematics during melt generation by intrusion of basalt into continental crust: Contributions to Mineralogy and Petrology, 136, 3, 285-295.

Labarthe-Hernández,G., Aguillón-Robles, A. Tristán-González, M., Jiménez-López, S., Romero,A., 1989, Cartografía geológica 1:50,000 de las hojas El Refugio y mineral el Realito, estados de San Luis Potosí y Guanajuato: Universidad Autónoma de San Luis Potosí, Instituto de Geología , Folleto Técnico 112, 76 p.

Lang, B., Steinitz, G., Sawkins, F. J., Simmons, S. F., 1988, K-Ar age studies in the Fresnillo silver district, Zacatecas, Mexico: Economic Geology, 83, 1642-1646.

Le Maitre, R.W., Bateman, P., Dudek, A., Keller, J., Lameyre, J., LeBas, M.J., Sabine, P.A., Schmid, R., Sorensen, H., Streckeisen, A., Wooley, A.R., Zanettin, B., 1989, Classification of Igneous Rocks and Glossary of Terms: Oxford, Blackwell, 193 p.

Ludwig, K.J., 2003, Isoplot 3.00: Berkeley Geochronology Center, Special Publication No. 4, 70 p.

Machado, M.L., 1970, Estudio Geológico del distrito minero La Paz: México, Instituto Politécnico Nacional, Escuela Superior de Ingeniería y Arquitectura, B. Sc. Thesis , 78 p

Malihan, T.D., 1987, The gold rich Dizon porphyry copper mine in the western central Luzon Islan, Philippines: Its geology and tectonic setting: Parkville, Victoria, Australia, Proceedings of the Pacific Rim Congress 87, Australasian Institute of Mining and Metallurgy, 303-307.

Martin, H., 1999, The adakitic magmas: modern analogues of Archean granitoids: Lithos, 46, 3, 411-429.

Martin, H., Moyen, J.F., 2003, Secular changes in TTG composition: comparison with modern adakites, *in* European Geophysical Society-American Geophisical Union-European Union of Geosciences joint assembly, Nice, April: Geophysical Research Abstracts, 5, 02673.

Martin, H., Smithies, R., Rapp, R., Moyen, J.F., Champion, D., 2005, McKenzie, D., 1984, An overview of adakite, tonalite-trondhjemite-granodiorite (TTG), and sanukitoid: relationships and some implications for crustal evolution: Lithos, 79(1-2), 1-24.

Megaw, P.K.M., Ruiz, J., Titley, S.R., 1988, High-temperature, carbonate-hosted Ag-Pb-Zn(Cu) deposits of northern Mexico: Economic Geology, 83(8), 1856-1885.

Megaw, P.K.M., Ruiz, J., Titley, S.R., 1988, High-temperature, carbonate-hosted Ag-Pb-Zn(Cu) deposits of Northern Mexico: Economic Geology, 83, 1856-1885.

Meinert, L.D., 1995, Igneous petrogenesis and skarn deposits: Geological Association of Canada, Special Paper 40, 569-583.

Meschede, M., Frisch, W., Uwe, R.H., Ratschbacher, L., 1997, Stress transmission across an active plate boundary: an example from southern Mexico: Tectonophysics, 266, 81–100.

McKenzie, D., 1984, The generation and compaction of partially molten rock: Journal of Petrology, 25(3), 713-765.

Mungall, J.E., 2002, Roasting the mantle: Slab melting and the genesis of major Au and Au-rich Cu deposits: Geology, 30(10), 915-918.

Mújica-Mondragón, M.R., Jacobo-Albarrán, J.J., 1983, Estudio petrogenético de las rocas ígneas y metamórficas del Altiplano Mexicano: México, Instituto Mexicano del Petróleo, Proyecto C-1156, unpublished report.

Muir, R.J., Weaver, S.D., Bradshaw, J.D., Eby, G.N., Evans, J.A., 1995, Geochemistry of the Cretaceous Separation Point Batholith, New Zealand: granitoid magmas formed by melting of mafic lithosphere: Journal of the Geological Society of London, 152, 689–701.

Nieto-Samaniego, A.F., Ferrari, L., Alaniz-Álvarez, S.A., Labarthe-Hernández, G., Rosas-Elguera, J., 1999, Variation of Cenozoic extensión and volcanism across the southern Sierra Madre Occidental volcanic province, Mexico: Geological Society of American Bulletin, 111, 347-363.

Nieto-Samaniego, A.F., Alaniz-Álvarez, S.A., Camprubí i Cano, A., 2005, La mesa Central de México: estratigrafía, estructura y evolución tectónica cenozoica: Boletín de la Sociedad Geologica Mexicana, 57(3), 285-318.

Orozco-Esquivel, M.T., Nieto-Samaniego, A.F., Alaniz-Álvarez, S.A., 2002, Origin of rhyolitic lavas in the Mesa Central, Mexico, by crustal melting related to extension: Journal of Volcanology and Geothermal Research, 118, 37-56.

Oyarzun, R., Márquez, A., Lillo, J., López, I., Rivera, S., 2001, Giant versus small porphyry copper deposits of Cenozoic age in northern Chile: adakitic versus normal calc-alkaline magmatism: Mineralium Deposita, 36,794-798.

Petford, N., 1995, Segregration of tonalitic-trondhjemitic melts in the continental crust: The mantle connection: Journal of Geophysical Research, 100, B8, 15735-15744.

Petford, N., Atherton, M., 1996, Na-rich partial melts from newly underplated basaltic crust: the Cordillera Blanca batholith, Peru: Journal of Petrology, 37, 1491-1521.

Prouteau, G., Scaillet, B., Pichavant, M., Maury, R.C., 1999, Fluid-present melting of oceanic crust in subduction zones: Geology, 27, 1111-1114.

Pupin J.P., 1992, Zircon from oceanic and continental granites: coupled study typology -trace element geochemistry: Bulletin de la Société Géologique de France, 163, 495-507.

Rabbia, O.M., Hernández, L.B., King, R.W., López-Escobar, L., 2002, Discussion on ''Giant versus small porphyry copper deposits of Cenozoic age in northern Chile: adakitic versus normal calc-alkaline magmatism'' by Oyarzun *et al.* (Mineralium Deposita 36:794–798, 2001): Mineralium Deposita, 37, 791-794.

Rapp, R., Watson, E., 1995, Dehydration melting of metabasalt at 8–32 kbar: Implications for continental growth and crust-mantle recycling: Journal of Petrology, 36(4), 891-931.

Rapp, R.P., Watson, E.B., Miller, C.F., 1991, Partial melting of amphibolite/eclogite and the origin of Archean trondhjemites and tonalites: Precambrian Research, 51, l–25.

Rapp, R.P., Shimizu, N., Norman, M.D., Applegate, G.S., 1999, Reaction between slab-derived melts and peridotite in the mantle wedge: experimental constraints at 3-8 GPa: Chemical Geology, 160, 335–356.

Rapp, R.P., Xiao, L., Shimizu, N., 2002, Experimental constraints on the origin of potassium-rich adakite in east China: Acta Petrologica Sinica, 18, 293–311.

Reich, M., Parada, M.A., Palacios, C., Dietrich, A., Schultz, F., Lehmann, B., 2003, Adakite-like signature of Late Miocene intrusions at the Los Pelambres giant porphyry copper deposit in the Andes of central Chile: metallogenic implications: Mineralium Deposita, 38(7), 876-885.

Richards, P., 2002, Discussion on ''Giant versus small porphyry copper deposits of Cenozoic age in northern Chile: adakitic versus normal calc-alkaline magmatism'' by Oyarzun *et al.* (Mineralium Deposita 36:794–798, 2001): Minereralium Deposita, 37, 788-790.

Rudnick, R.L., Cameron, L.C., 1991, Age diversity of the deep crust in northern Mexico: Geology, 19(12), 1197-1200.

Rushmer, T., 1996, Partial melting of two amphibolites: contrasting experimental results under fluid-absent conditions: Contribution to Mineralogy and Petrology, 107, 41-59.

Sajona, F.G., Maury, R.C., Pubellier, M., Leterrier, J., Bellon, H., Cotten, J., 2000, Magmatic source enrichment by slab-derived melts in a young post-collision setting, central Mindanao (Philippines): Lithos, 54(3-4), 173-206.

Sawkins, F.J.,1990, Metal deposits in relation to plate tectonics: Berlin, Springer, 2nd. ed., 461.

Schmid, C., Goes, S., van der Lee, S., Giardini, D., 2002, Fate of the Cenozoic Farallon slab from a comparison of kinematic thermal modeling with tomographic images: Earth and Planetary Science Letters, 204, 17-32

Sen, C., Dunn, T., 1994, Dehydration melting of a basaltic composition amphibolite at 1.5 and 2.0 GPa: implications for the origin of adakites: Contribution to Mineralogy and Petrology, 117, 394-409.

Skjerlie, K.P., Patino-Douce, A.E., 2002, The fluid-absent partial melting of a zoisite-bearing quartz eclogite from 1.0 to 3.2 GPa: implications for melting in thickened continental crust and for subduction-zone processes: Journal of Petrology 43, 291–314.

Sillitoe, R.H., 1997, Characteristics and controls of the largest porphyry copper-gold and epithermal gold deposits in the circum-Pacific region: Australian Journal of Earth Sciencas, 44(3), 373 - 388.

Sillitoe, R.H., Gappe, I.M.,1984, Philippine Porphyry Deposits: Geologic settings and Characteristics: Bankok, United Nations Economic and Social Commission for Asia and the Pacific, CCOP technical publications,14-89.

Silva-Romo, G., 1996, Estudio de la estratigrafía y estructuras tectónicas de la Sierra de Salinas, Estados de San Luis Potosí y Zacatecas: Universidad Nacional Autónoma de México, Facultad de Ciencias, División de Estudios de Posgrado, M. Sc. Thesis, 139 p.

Silva-Romo, G., Arellano-Gil, J., Mendoza-Rosales, C., Nieto-Obregón, J., 2000, A submarine fan in the Mesa Central, Mexico: Journal of South American Earth Sciences, 13, 429-442.

Simmons, S.F., 1991, Hydrologic implications of alteration and fluid inclusion studies in the Fresnillo District, Mexico. Evidence for a brine reservoir and a descending water table during the formation of hydrothermal Ag-Pb-Zn ore bodies: Economic Geology, 86, 1579-1601.

Skewes, M.A., Stern, C.R., 1994, Tectonic trigger for the formation of late Miocene Cu-rich breccia pipes in the Andes of central Chile: Geology, 22, 551-554.

Spurr, J.E., Garrey, G.H., Fenner, C.N., 1912, Study of a contact metamorphic ore deposit. The Dolores Mine, at Matehuala, S.L.P., Mexico: Economic Geology, 7, 444-484.

Stacey, J.S., Kramers, J.D., 1975, Approximation of terrestrial lead isotope evolution by a two-stage model: Earth and Planetary Science Letters, 26, 207.

Stern, C.R., Kilian, R., 1996, Role of the subducted slab, mantle wedge and continental crust in the generation of adakites from the Andean Austral Volcanic Zone: Contributions to Mineralogy and Petrology, 123(3), 263-281.

Thieblemont, D., Stein, G., Lecuyer, J.L. 1997, Gisements épithermaux et porphyriques: la connexion adakite: Comptes Rendus de l'Académie des Sciences Paris, Series IIA, 325, 103-109.

Tristán-González, M., 1986, Estratigrafía y tectónica del graben de Villa de Reyes en los estados de San Luis Potosí y Guanajuato, México: Universidad Autónoma de San Luis Potosí, Instituto de Geología, Folleto Técnico, 107, 91.

Tuta, Z.H., Sutter, J.F., Kesler, S.E., Ruiz, J., 1988, Geochronology of mercury, tin, and fluorine Mineralization in Northern Mexico: Economic Geology, 83, 1931-1942.

Valencia-Moreno, M., Ochoa-Landín, L., Noguez-Alcántara, B., Ruiz, J., Pérez-Segura, E., 2006, Características metalogenéticas de los depósitos de tipo pórfido cuprífero en México y su situación en el contexto mundial: Boletín de la Sociedad Geológica de México, 58(1), 1-26.

Wang, Q., Xu, J.F., Zhao, Z.H., Bao, Z.W., Xu, W., Xiong, X.L., 2004, Cretaceous high-potassium intrusive rocks in the Yueshan–Hongzhen area of east China: adakites in an extensional tectonic regime within a continent: Geochemical Journal, 38, 417–434.

Wang, Q., Xu, J.F., Jian, P., Bao, Z.W., Zhao, Z.H., Li, C.F., Xiong, X. L., Ma, J.L., 2006, Petrogenesis of adakitic porphyries in an

extensional tectonic setting, Dexing, South China: Implications for the genesis of porphyry copper mineralization: Journal of Petrology, 47(1), 119-144.

Wiedenbeck, P., Alle, F., Corfu, W.L., Griffin, M., Meier, F., Oberli, A., Von Quadt, J.C., Roddick W., Spiegel, M., 1995, Three natural zircon standards for U-Th-Pb, Lu–Hf, trace element and REE analyses: Geostandards Newsletter 19, 1-24.

Xiong, X.L., Li, X.H., Xu, J.F., Li, W.X., Zhao Z.H., Wang, Q., Chen, X.M., 2003, Extremely high-Na adakite-like magmas derived from alkali-rich basaltic underplate: the Late Cretaceous Zhantang andesites in the Huichang Basin, SE China: Geochemical Journal 37, 233–252.

Xu, J.F., Shinjio, R., Defant, M.J., Wang, Q., Rapp, R.P., 2002, Origin of Mesozoic adakitic intrusive rocks in the Ningzhen area of east China: partial melting of delaminated lower continental crust?: Geology, 12, 1111–1114.

Zhang L.C., Xiao, W.J., Qin, K.Z., Zhang, Q., 2005, The adakite connection of the Tuwu-Yandong copper porphyry belt, eastern Tianshan, NW China: trace element and Sr-Nd-Pb isotope geochemistry: Mineralium Deposita, 41(2), 188-200.

Manuscript received: June 11, 2007
Corrected manuscript received: October 9, 2007
Manuscript accepted: October 12, 2007